Examining the Viability of Air Quality Index as a Primary Proxy for Aquatic Industrial Pollution: A Case Study of South Korea's Han and Austria's Donau River

Jiwoo Jung[a], Leon Plakolm[b*]
[a]The American International School of Vienna, Salmannsdorfer Strasse 47, 1190 Vienna, Austria
[b]University of Vienna, Josef-Holaubek-Platz 2, 1090 Vienna, Austria

Abstract

Globally, billions of people continue to suffer from the contamination of water bodies with its scale and degree of impact ever-increasing. Yet, compared to the hundreds of thousands of rivers existing worldwide, the extent of studies done to analyze the water quality of rivers appear miniscule. As industrialization continues to predominantly contaminate the surface water of river flows, examination of water bodies becomes increasingly dire. This research compares and evaluates the industrial pollution within the Han River of South Korea and the Donau River of Austria, interpreting the independently collected data of water parameters of dissolved oxygen, pH and total dissolved solids while reviewing existing information regarding the two rivers, both quantitative and qualitative. Public data human population density and air quality index (AQI) was also utilized. Using cumulative AQI, All data revealed the exacerbating level of industrial pollution within the Han River in contrast to the Donau River experiencing manageable degree of contamination. The data were used to create matrices of Pearson's correlation coefficients as well, of which the matrix cumulatively evaluating the data collected showed strong correlation between all pairs of the parameters examined, further validating the evaluation of the industrial pollution among both rivers. The data was used for training and testing supervised machine-learning models in Python, applying various layers of feature selection. Data from public databases were gathered to create linear, nonlinear support vector regressor and model ensembles, applying k-fold Cross Validation in addition to distinguishing between feature selection and dimensionality reduction to ensure high accuracy.

Keywords: environmental science, ecology, river hydrology, industrial pollution, machine learning

* Corresponding author.
E-mail address: leonp01@unet.univie.ac.at (L. Plakolm)

1. Introduction

The rise in global pollution poses significant risks to both ecosystems and modern society. The contamination of rivers complicates the current cultural, economic, and political dynamics among human populations. Rivers foster unique biodiversity patterns that help mitigate the detrimental effects of human activities (Blanchet et al., 2020). Moreover, while rivers facilitate hydrologic, geomorphic, and ecological connectivity, they also play a crucial role in transferring organisms and sustaining biodiversity through the cycling of water. As global civilization increasingly urbanizes, the social connections among human populations become even more pronounced (Kondolf & Pinto, 2016). Additionally, river and environmental flows serve as a means to mitigate the impacts of anthropogenic activities, directly linking cultural values and lifestyles of communities while also protecting and restoring aquatic ecosystems (Anderson et al., 2019).

Water pollution is the contamination of water bodies, including rivers, lakes, oceans, groundwater, and even aquifers, by harmful substances, critically affecting the human population by placing human health, ecosystem, and the availability of water at risk (Mohamed, 2024). Affecting river flows as well, numerous aquatic systems around the world experience degradation as environmental flows become compromised despite its growing importance. Such degradation raises the urgency to maintain the water quality of rivers and environmental flows (Anderson et al., 2019). Since water is a fundamental aspect of the environment that provides important benefits for the human population, the management of water quality is essential: “Water is life without pollution, but death when it is polluted” (Igwe et al., 2017). The immediate call to action presents a crucial need to reduce the harm caused by water pollution to the ecosystem and human health. Among the two million people dying each year due to diarrhoeal illnesses, substandard sanitation of drinking water has led to approximately 90% of such deaths (Lin et al., 2022).

To discuss the pollutants of river pollution, anthropogenic activities such as agriculture appear to bring contamination and subsequent pollution to our varied ecosystems (Bashir et al., 2020). 38% of the streams extending across European nations are “significantly under agricultural pressure”; in the United States, agriculture is one of the primary sources of pollution within rivers and wetlands; agriculture has resulted in severe surface-water pollution and groundwater pollution of Chinese rivers (Bashir et al., 2020). These anthropogenic activities have resulted in the contamination of water sources through forms of bacteria and viruses, which are known as emerging pathogens due to their apparent virulence: pesticides, sludges, and sewages contaminated the soils of rivers and provided industrial discharges of chemicals and microelements, also becoming emerging pollutants of the environment and water bodies following industrialization (Mishra et al., 2023).

Among these sources of water pollution, industrial pollution is a leading cause within rivers:
globally, numerous people perceive and utilize water bodies as an “industrial dustbin” for discarding industrial effluents without bearing the extreme environmental cost (Igwe et al.,

2017). It is the negative externality of industries avoiding corporate social responsibilities that continues to aggravate the problematic effect of industrial pollution. Sewage is the greatest volume of waste discharged into the aquatic ecosystems, of which the majority originate from industrial practices: as industries emit 80% of municipal wastewater into river bodies without filtration, millions of tons of heavy metals and toxic sludge eventually reach river bodies (Bashir et al., 2020). When exemplifying the case study on the Ganga River, bioaccumulation and biomagnification from industrialization and urbanization have placed human health and welfare in danger, highlighting the necessity for reducing industrial effluent released into the Ganga River (Roy & Shamim, 2020).

The assessment of water quality is significant in determining the level of pollution within an area and understanding its impacts; to calculate and quantify water quality, specific parameters of waters are measured. Conventionally, the water quality of a water body is considered to be accurately determined through a 'water quality index', or a WQI. In a study of 30 different WQIs and their characteristics, the indices are able to be organized into three categories: a fixed system of parameters, an open system where basic parameters are recommended but not limited to, and a mixed system in which consists of both basic and additional parameters (Sutadian et al., 2015). An observation could be deduced from the comparison that the nearly all WQIs commonly included parameters such as potential for Hydrogen (pH), Dissolved Oxygen (DO), Biochemical Oxygen Demand (BOD), Chemical Oxygen Demand (COD) and Total Solids (TS) (Sutadian et al., 2015). These physicochemical and biological parameters, according to multiple authors, vary seasonally. Moreover, anthropogenic activities, soil erosion and waste deposited into rivers have been identified as factors influencing one or more of the parameters, showcasing that a multitude of variables are able to affect the measurements of the parameters (Igwe et al., 2017). To interpret individually, Total Dissolved Solids (TDS), a particular type of TS, includes substances from domestic and industrial waste as well, resulting in a positive correlation with industrialization (Rusydi, 2018); the case study in Medlock River of Great Manchester, United Kingdom revealed the negative correlation between DO levels industrial land and a positive relationship with woodlands, whereas BOD had increased in concentration when wastewater was discharged into the river (Nguyen et al. et al., 2023); COD concentration had risen in the Anzali Wetland, Iran due to seasonal climate change (Tahershamsi et al., 2009); lastly, a decrease in the pH values could be observed in the Guadiamar River following the 1998 Aznalcóllar spill in Andalusia, Spain that raised the toxicity of the water, revealing a connection between pH and industrial discharges as well (M. Olías et al., 2005).

The Han River runs throughout South Korea and passes through multiple cities, from the riverhead Geomryongso, Taebaek to the Yellow Sea. It is a significant aspect of South Korea, supplying clean water to over 20 million people solely within Seoul, the nation's capital (Lee et al., 2019). Occupying a watershed area of 26200 km^2, the Han River has been straightened to be of 469.7 km in length for water control and presents a diverse ecosystem that should be maintained; yet the continual reduction in species such as the Korean eel (*Anguilla japonica)* indicates the threat faced by its ecosystem due to environmental degradation and pollution (Lee et al., 2019). The Han River is also extremely significant in the cultural context by providing aid

throughout the development and settlement of the Korean civilization in addition to the economic benefits a long, controlled river provides (Lee et al., 2019).

The management of the Han River is strictly managed by the South Korean government, as the river is an essential aspect of the nation. Subsequent to the industrialization of the nation, the government had recognized the importance of water quality management and undertook “multi-purpose dam” construction projects in the upstream region of the Han River while enacting five new regulations to protect the river (Shin et al., 2016). However, the management of the Han River has been increasing in difficulty as the water quality of the river body appeared to deteriorate. In particular, the eutrophication of the Han river is a substantial concern when managing the river’s water quality: the decline in BOD/COD ratio between 1986 and 2006 displays the increase in the proportion of recalcitrant organic matter, suggesting of a possibility of eutrophication of the river exacerbating(Shin et al., 2011). On the contrary, a decreasing trend of BOD levels could be observed due to the newly implemented sewage treatment facilities (Shin et al., 2011). Such evolved methods of regulation of the environment have begun to emerge in South Korea, invoked by the heightening of the pollution levels. As one of the selected procedures since the 1970s, Integrated Water Resource Management (IWRM) approaches are environmentally sustainable and considers human necessities (Hwang et al., 2020). Clearly illustrated by this study, methods of measuring and maintaining water quality become increasingly important as the consequential effects of environmental pollution become more drastic and complex.

The Donau River extends through numerous European nations, beginning in the Black Forest mountains of Germany and flowing until reaching the Black Sea. It is similarly significant to Austria as the second-largest river in Europe, stretching over a great distance of 2,845 km and critically influencing the ecological and economical landscape (Dávid & Madudová, 2019). Providing residence for diverse species of flora and fauna including endangered animals, the Donau river’s biodiversity appears to consist of over 320 avian species and a larger distinction among reptiles and amphibians (Vynokurova et al., 2023). The Danube River contributed to shaping the culture of Austria through various characteristics, allowing for “cultural, ethnic and political diversity” within the Donau River Basin (Schmid et al., 2023).

Similar to the Han River, the Austrian government provides management of the Donau River, but numerous organizations have implemented various ways of preserving it. The European Union’s enactment of the Water Framework Direction (WFD) exemplifies such involvement, proposing guidelines for a vast majority of European nations to follow (Stagl & Hattermann, 2015). Even so, as the urbanization of the nation continues, its environment continues to be damaged: within the last two centuries, the floodplain of the river has declined to less than 19% of the original size, demonstrating a decrease from 41605 km^2 to 7845 km^2 (Habersack et al., 2015). This decrease is detrimental, since most countries adjacent to the Donau River Basin generate over 45% of their hydropower through the Donau River Basin (Habersack et al., 2015). Furthermore, the contamination of the river’s water itself presents a further significant impact. The pollution of the river causes changes to the hydrodynamics of the river and restricts the spawning areas of a great number of species (Habersack et al., 2015).

Consistent sampling of water quality is extremely important in long-term safeguarding of river bodies, providing a quantitative measurement of the river's pollution, consequences of industrial discharge, and the effect of urbanization. Numerous research emphasizes the importance of monitoring the water quality of rivers that reveals their current state. "Regular review of environmental effects of surface water pollution should be conducted by researchers to indicate the trend in pollutional loads of rivers, stream and lakes across the globe" (Igwe et al., 2017); "the evaluation of biological diversity have been recognized as an important national task to establish bio-sovereignty in the world" (Lee et al., 2019); "The paper emphasizes the importance of ensuring safe and clean drinking water through robust water treatment and monitoring systems" (Mohamed, 2024). Considering the implication above, this paper showcases a comparison of water quality and the effect of industrial pollution on the Han and Donau River, allowing important conclusions to be drawn from the two rivers located in hugely distinct settings. The research utilizes the parameters of DO, pH and TDS within the river bodies to evaluate the water quality of the Han and Donau River, supported with identified factors of industrial pollution.

2. Study area, materials and methods

2.1 Geographical setting

The data collection for the Han River was focused exclusively on the vicinity of Seoul. In a similar manner, this study gathered data from the region of Vienna. The selection of data collection sites was constrained by geographical challenges; thus, the Han and Danube Rivers were categorized into three segments: upstream, midstream, and downstream. The rivers' streams were respectively trisected from the center of Seoul, South Korea and Vienna, Austria, with an approximate unit distance of 20 km between the data collection sites. Specifically, two sites of each stream were homogeneously selected to be directly opposite of one another as a means to account for variations in the collected data due to soil erosion, water flows, and geological settings. The sites were selected based on accessibility, as the majority of the river basin was limited in access. Hence, the selected sites slightly differed in terms of collecting DO, pH, and TDS. Since elevation is a primary variable that influences the physicochemical parameters of a river body, the altitude of the sites from sea level was recorded through a mobile application. The elevation of the data sites appeared consistent and there was minimal difference between the two rivers. Another factor to consider is the temporal setting of data collection. The DO data was collected during August and September of 2023; TDS and pH data were collected between the end of June and the beginning of August 2024. Thus, all data was collected during wet seasons, in which elements such as rain and temperature can cause volatility in the data reading that should be accounted for. The setting of data collection sites is summarized in Table 1. The specific geological area of data collection is displayed in Figure 1.

Table 1. Setting of data collection sites.

	Han						Donau					
River Section	Upstream		Midstream		Downstream		Upstream		Midstream		Downstream	
Cardinal Direction of River Bank	North	South	North	South	North	South	North-east	South-west	North-east	South-west	North	South
Position of River Curve	Inner-most	Outer-most	Outer-most	Inner-most	Outer-most	Inner-most	Inner-most	Outer-most	Inner-most	Outer-most	Outer-most	Inner-most
Data Sites of DO Data	Wabu Eup	Cheon-hyeon Dong	Yong-san Gu	Seocho Gu	Mapo Gu	Yeong-deung-po Gu	Korneu-burg	Kloster-neuburg	Donau-stadt	Leopold-stadt	Orth an der Donau	Haslau-Maria Ellend
Data Sites of pH & TDS Data	Wabu Eup	Cheon-hyeon Dong	Gwang-jin Gu	Gang-nam Gu	Mapo Gu	Yeong-deung-po Gu	Korneu-burg	Kloster-neuburg	Donau-stadt	Brigitt-enau	Orth an der Donau	Haslau-Maria Ellend
Altitude From Sea Level (m)	11	17	-2	-3	-3	-3	155	157	142	137	136	139

Figure 1. Maps of DO data collection sites in Han river (1a) and Donau river (1b) and pH and TDS data collection sites in Han river (1c) and Donau river (1d)

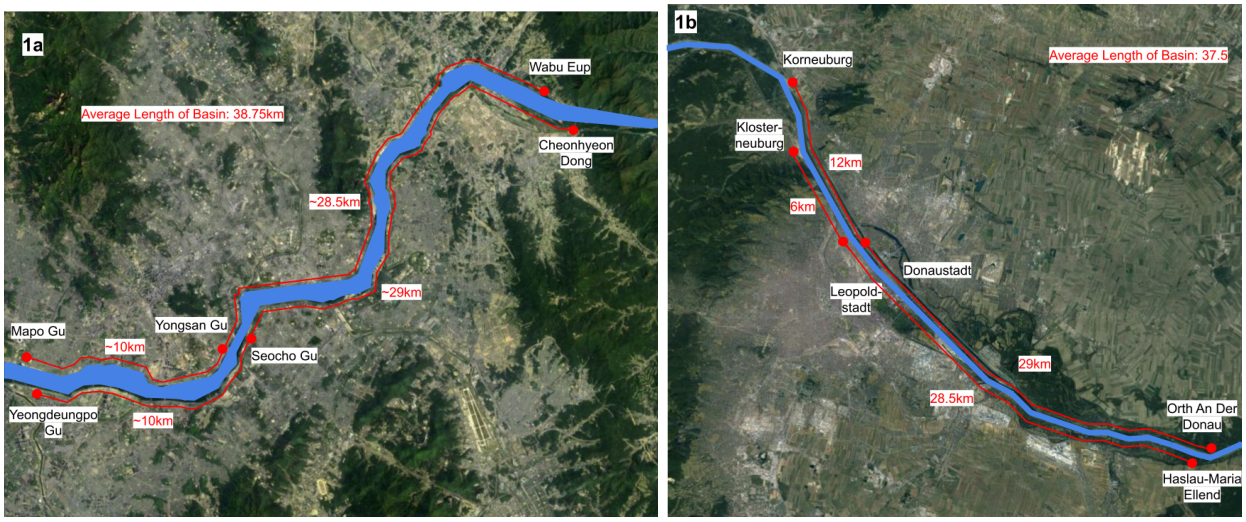

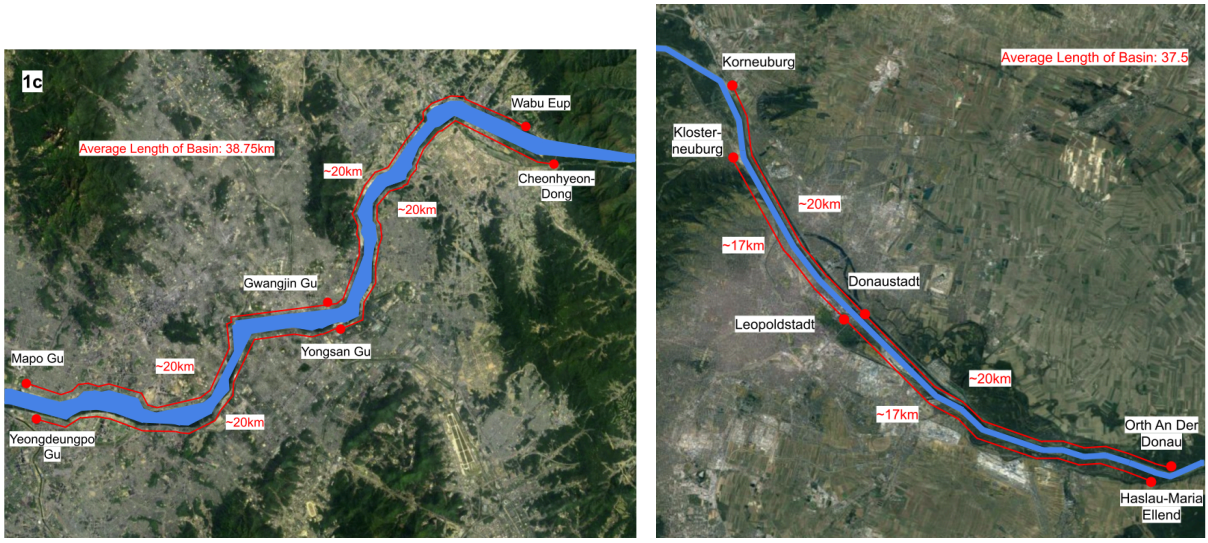

Footnote: Google satellite images used (Google Maps, 2019)

2.2 Data collection

The data was collected using a hand-crafted telescopic rod, which facilitated the gathering of 100 mL samples of surface water from the rivers at a depth of 5 meters at each data collection point. For measuring dissolved oxygen (DO), a Milwaukee Dissolved Oxygen Meter was employed, while pH and Total Dissolved Solids (TDS) were measured using **Virph Digital Water pH TDS Temperature Meter.** A digital water thermometer (CAS) was utilized to record the temperature of the samples. DO measurements were collected at one-minute intervals and recorded ex-situ within three days of data collection, resulting in 150 trials of data for each site. During the collection of pH and TDS data, values were consistently recorded by two sensors every 30 seconds for 75 trials each, minimizing fluctuations in the data and allowing for in-situ collection due to the shorter interval and reduced number of trials. The dates of sample and data collection were documented and are presented in Tables 2 and 3.

Table 2. Date of DO samples and data collection.

	Han						Donau					
Stream	Upstream		Midstream		Downstream		Upstream		Midstream		Downstream	
Site	Wabu Eup	Cheon-hyeon Dong	Yong-san Gu	Seocho Gu	Mapo Gu	Yeong-deung-po Gu	Korneu-burg	Klost-neu-burg	Donau-stadt	Leo-pold-stadt	Orth an der Donau	Haslau-Maria Ellend
Sample Collection	Aug. 4	Aug. 4	Aug. 7	Aug. 7	Aug. 6	Aug. 6	Sep. 16	Sep. 7	Aug. 29	Aug. 25	Sep. 2	Sep. 9
Data Collection	Aug. 5	Aug. 5	Aug. 9-10	Aug. 9-10	Aug. 6	Aug. 6	Sep. 16	Sep. 9	Aug. 31	Aug. 25-26	Sep. 2-3	Sep. 10

Table 3. Date of pH and TDS samples and data collection.

	Han						Donau					
Stream	Upstream		Midstream		Downstream		Upstream		Midstream		Downstream	
Site	Wabu Eup	Cheon-hyeon Dong	Gwang-jin Gu	Gang-nam Gu	Mapo Gu	Yeong-deung-po Gu	Korneu-burg	Klost-neu-burg	Donau-stadt	Brigit-teau	Orth an der Donau	Haslau-Maria Ellend
Sample Collection	Jul. 13	Jul. 15	Jul. 12	July. 14	Jun. 30	Jun. 30	Aug. 17	Aug. 17	Aug. 17	Aug. 17	Aug. 19	Aug. 19
Data Collection												

2.3 Modelling Methodology

In the study, three types of models were implemented in an attempt to identify the most accurate model for predicting industrial pollution based on various parameters: linear, support vector and ensemble. The Python library Scikit-Learn has been utilized for this research where multiple base models, feature selection methods and dimensionality reduction techniques are provided (Buitinck et al, 2013).

3. Results and Discussion

3.1 Qualitative factors of industrial pollution

When perceiving the qualitative variables of industrial pollution, various factors contribute towards the overall contamination: for instance, a case study of the Karnafully River in Bangladesh identified pesticides, solid wastes and leakages as the primary pollutants of the river originating from nearby industries (Bhuyan & Islam, 2017). Another paper investigating the Ipojuca River in Brazil underscores the sugarcane factories raising the temperature of the water, organic acids exacerbating the river and excess potassium from fertigation fluids, resulting in the river being contaminated with biodegradable matter (Gunkel et al., 2006). Such inquiries highlight that a multitude of qualitative factors must be considered when examining industrial pollution.

In South Korea, the Han River has experienced the greatest number of contamination among the major rivers within the nation, accumulating to 283 cases between 2014 and 2018 (Jung, 2019). Over the course of the past five years, 5494873 m^3 of sewage was produced daily by the 24263 active plants, of which 3823429 m^3 was disposed in the Han River (Research Report - Research on the establishment of a conservation plan for the Han River Estuary Wetland Protection Area (20-24)). The sewage accumulates to be 11 million tons as wastewater being treated, which surpasses the legal restriction by 5 million tons of sewage (An, 2022). Such contamination also led to the Han River being ranked as the 43rd highest drug contaminated river among water bodies from 137 different countries (Cho, 2023). The declining water quality has been highlighted as a significant concern since the 1960s, when South Korea began

industrialization (Kim & Seoul National University Graduate School of Environmental Studies, 2024). Such information establishes the Han River as a body of water highly polluted by industrial pollution.

Contrastingly, Austria's Donau River seemingly suffers from industrialization to a minor degree: an evaluation from 2009 deemed 22% of the river as in ecologically good condition and 45% achieved good chemical status (Gasparotti, 2014). However, a study hypothesizing the independence of factories from the Donau River with continuing industrialization was disproven as the river's water quality deteriorated with industries being able to transport their waste into the Donau River from a greater distance (Radu et al., 2020). This conclusion provides a counterclaim to the Donau River being generally less contaminated. Nonetheless, 97.7% of the nation's water has been determined to be excellent in quality (International Commission for the Protection of the Danube River, 2022). The effort of the European Union to improve the water quality of the river has allowed the water to be safe for activities such as swimming (International Commission for the Protection of the Danube River, 2021). Hence, a multitude of evidence suggests the Donau River's comparatively less extent of industrial pollution than the Han River.

3.2 Environmental variables

The surface water sample temperatures recorded during the collection of dissolved oxygen (DO) data in 2023 varied between 22.6°C and 29.2°C, with a maximum temperature fluctuation of 4.3°C at each site. Overall, the temperature showed a trend of either increasing or decreasing until reaching approximately 25°C. In 2024, during the collection of pH and total dissolved solids (TDS) data, the temperatures ranged from 24.5°C to 30.5°C. The maximum temperature variation observed per site was slightly higher than the previous year, measuring 4.7°C.

3.3 Physicochemical parameters

The mean, standard deviation(SD) and standard error of the mean(SE Mean) of the selected parameters for the water samples were presented in Tables 4 to 7. The DO value was narrowly within the tolerable range of 6.5 to 8 mg/L, the minimum being 6.660 mg/L and maximum being 7.709 mg/L; the pH varied between 7.496 and 7.643; lastly, TDS ranged from 83.912 to 196.628 ppm.

Tables 4-7. Statistical summary of river parameters.

River	Han River																	
Stream	Upstream						Midstream						Downstream					
Location	Wabu Eup			Cheonhyeon Dong			Yongsan Gu			Seocho Gu			Map -Gu			Yeongdeungpo Gu		
	μ	SE μ	SD	μ	SE μ	SD	μ	SE μ	SD	μ	SE μ	SD	μ	SE μ	SD	μ	SE μ	SD
DO(mg/L)	6.918	0.014	0.171	6.975	0.015	0.185	6.818	0.011	0.137	6.799	0.012	0.141	6.713	0.011	0.141	6.660	0.012	0.142
μDO (mg/L)	6.814																	

River	Donau River																	
Stream	Upstream						Midstream						Downstream					
Location	Korneuburg			Klosterneuburg			Donaustadt			Leopoldstadt			Orth an der Donau			Haslau-Maria Ellend		
	μ	SE μ	SD	μ	SE μ	SD	μ	SE μ	SD	μ	SE μ	SD	μ	SE μ	SD	μ	SE μ	SD
DO(mg/L)	7.628	0.009	0.108	7.709	0.011	0.133	7.476	0.014	0.171	7.549	0.013	0.164	7.360	0.011	0.130	7.292	0.009	0.108z
μDO (mg/L)	7.502																	

River	Han River																	
Stream	Upstream						Midstream						Downstream					
Location	Wabu Eup			Cheonhyeon Dong			Gwangjin Gu			Gangnam Gu			Mapo Gu			Yeongdeungpo Gu		
	μ	SE μ	SD	μ	SE μ	SD	μ	SE μ	SD	μ	SE μ	SD	μ	SE μ	SD	μ	S Eμ	S D
pH	7.748	0.008	0.094	7.781	0.002	0.029	7.560	0.007	0.090	7.740	0.002	0.028	7.496	0.048	0.581	7.567	0.002	0.028
μpH	7.649																	
TDS (ppm)	95.899	0.127	1.551	103.831	0.076	0.929	83.912	0.080	0.975	102.473	0.109	1.327	110.642	0.061	0.747	117.284	0.044	0.535
μTDS (ppm)	102.340																	

River	Donau River																	
Stream	Upstream						Midstream						Downstream					
Location	Korneuburg			Klosterneuburg			Donaustadt			Leopoldstadt			Orth an der Donau			Haslau-Maria Ellend		
	μ	SE μ	SD	μ	SE μ	SD	μ	SE μ	SD	μ	SE μ	SD	μ	SE μ	SD	μ	SE μ	SD
pH	8.455	0.002	0.019	8.352	0.002	0.019	8.646	0.000	0.006	8.540	0.002	0.023	8.570	0.001	0.008	8.643	0.001	0.018
μpH	8.534																	
TDS (ppm)	191.318	0.081	0.990	196.628	0.142	1.723	154.622	0.086	1.046	191.541	0.213	2.593	192.507	0.069	0.837	188.108	0.062	0.757
μTDS (ppm)	185.787																	

The statistical summary reinforces the claim that the level of industrial pollution in the Han River is severer than that of the Donau River. As conventionally known, low values of DO and TDS are associated with lower water quality and serious contamination of a river by signifying the

lack of resources aquatic life consumes to survive, and vice versa; the Han River presents lower mean DO and TDS values of 6.814 mg/L and 102.34 ppm in comparison to the Donau River's values of 7.502 mg/L and 185.787 ppm. Furthermore, pH represents the acidity of the water with **lower** values becoming more toxic, indicating contamination of the surface water; the mean pH value from the Han River of 7.649 is significantly lower than 8.534 from the Donau River. Both observations establish the Han River as being substantially polluted relative to the Donau River.

3.4 Human population density

Human population density (HPD) measures the number of inhabitants within a defined area and serves as an indirect indicator of the level of urbanization and industrialization in different regions. Notably, population density provides a quantitative estimate of industrial pollution: a study conducted in the Weihe River of China revealed a relationship between HPD and industrial point-source sewage (Zhang et al., 2012). Similarly, HPD has been linked to industrial emissions in the Mediterranean regions, where areas characterized by high population density are considered highly susceptible to severe pollution (Acar & Mahmut Tekce, 2014).Thus, as HPD can be utilized as a possible method of evaluating industrial pollution, within the Han and Donau River, public data of HPD from and Austria Statistik was recorded in the data displayed in Tables 8 to 11. HPD values from 2021 were partly used as HPD during DO collection, since the Austrian government did not update the population of nearby regions of Vienna between 2021 and 2024.

Table 8. HPD of South Korean regions of DO data collection, 2021/2023

River	Han River					
Location	Wabu Eup	Cheonhyeon Dong	Yongsan Gu	Seocho Gu	Mapo Gu	Yeongdeungpo Gu
Year	2023	2023	2023	2023	2023	2023
HPD (ppl/km^2)	1,155	187	9,924	8,617	15,303	15,316
μHPD (ppl/km^2)	8,417					

Table 9. HPD of Austrian regions of DO data collection, 2021/2023

River	Donau River					
Location	Korneuburg	Kloster-neuburg	Donaustadt	Leopoldstadt	Orth an der Donau	Haslau-Maria Ellend
Year	2021	2021	2023	2023	2021	2021
HPD (ppl/km^2)	1,376	361	2,085	5,639	65	81
μHPD (ppl/km^2)	1,601					

Table 10. HPD of South Korean regions of pH and TDS data collection, 2024

River	Han River					
Location	Wabu Eup	Cheonhyeon Dong	Gwangjin Gu	Gangnam Gu	Mapo Gu	Yeongdeungpo Gu
Year	2024	2024	2024	2024	2024	2024
HPD (ppl/km^2)	1,160	173	19,587	14,090	15,221	15,277
μHPD (ppl/km^2)	10,918					

Table 11. HPD of Austrian regions of pH and TDS data collection, 2024

River	Donau River					
Location	Korneuburg	Kloster-neuburg	Donaustadt	Leopoldstadt	Orth an der Donau	Haslau-Maria Ellend
Year	2024	2024	2024	2024	2024	2024
HPD (ppl/km^2)	1,404	369	2,158	5,722	66	82
μHPD (ppl/km^2)	1,634					

Tables 8 to 11show that HPD is naturally higher in regions located within South Korea's capital Seoul and Austria's capital Vienna. All within Seoul, Yongsan Gu, Seocho Gu, Gwangjin Gu and Gangnam Gu each displayed the highest HPD values of the recorded regions with respective values of 9,924, 8,617, 19,587, and 14,090 ppl/km^2; similarly, Mapo Gu and Yeongdeungpo Gu are near the border of Seoul yet was highly populated. Situated in the center of Vienna, Donaustadt and Leopoldstadt also revealed HPD values of 2085 and 5639 ppl/km^2 in 2023 as well as 2158 and 5722 ppl/km^2 in 2024. The countryside regions of the two countries exhibited low values of HPD, ranging from 65 to 1160 ppl/km^2. The overall HPD in South Korea appears to have been significantly higher in South Korea than Austria during both 2021 with Han River's average HPD of 8417 and 10918 ppl/km^2 in contrast to Donau River's average HPD of 1601 and 1634 ppl/km^2, further highlighting the likelihood that the Han River has experienced greater levels of industrial pollution than the Donau River.

3.5 Air quality index

The air quality index (AQI) provides information and insight into the contamination of air within a certain region by measuring specific pollutants within the air. Therefore, AQI serves as an indicator of pollution and potential health risks (Wu et al., 2021). Common pollutants that AQI measures are PM_{10}, PM_{15}, sulfur dioxide, and carbon dioxide (Cairncross et al., 2007). Each of these pollutants is harmful to human health and collected data of such parameters are utilized to create a cumulative value known as AQI. While the basic Air Quality Index ranging from 0 to 500 is most commonly used, certain regions in the world utilize different AQI types and metrics

to evaluate the level of air quality and pollution within an area. Table 12 provides the AQI descriptors of South Korea and the European Union (EU), which includes Austria (Wu et al., 2021).

Table 12. AQI Descriptor of South Korea and EU

Countries/Regions	AQI Types	Level, Descriptor, Index Range	Target Groups in Warning Messages at Each Level
South Korea	CAI (Comprehensive Air-Quality Index)	A, Good, 0–50	(1) Patients (all) (2) Sensitive groups (C–E) (3) General public (C, E)
		B, Moderate, 51–100	
		C, Unhealthy, 101–250	
		D/E, Very Unhealthy, 251–500	
EU	EAQI (European Air Quality Index)	1, Good, (Each*)	(Separate warning messages for each population group) (1) At-risk individuals (2) General population
		2, Fair, (Each*)	
		3, Moderate, (Each*)	
		4, Poor, (Each*)	
		5, Very Poor, (Each*)	
		6, Extremely Poor, (Each*)	

As the AQI demonstrates an aspect of pollution within an area, public AQI data from the World Air Quality Index Project was utilized, separating the region of data collection by provinces and averaging the AQI values of the data collection date from the nearest station to the data collection sites. As the EU does not specifically provide which index values are utilized for calculating EAQI, the AQI descriptor from South Korea was utilized. PM2.5 and PM10 were the two selected parameters that are the most common pollutants measured by AQI and other parameters differed per data collection station. The CAI was calculated by selecting the highest value and adding 50 if both PM2.5 and PM10 are included in categories C,D, or E; else, the highest value was selected as the CAI(AirKorea: Introduction to the CAI, 2022). Tables 13 to 16 summarize the recorded public data from DO data collection in 2023 and pH & TDS data collection in 2024.

Table 13. AQI of South Korean regions of DO data collection, 2023 (WAQI, 2008)

River	Han River					
Date of sample collection	Aug. 4	Aug. 4	Aug. 7	Aug. 7	Aug. 6	Aug. 6
Location	Wabu Eup	Cheonhyeon Dong	Yongsan Gu	Seocho Gu	Mapo Gu	Yeongdeungpo Gu
AQI PM2.5	59.000	56.000	65.000	37.000	51.000	54.000

(μg/m^3)						
AQI PM10 (μg/m^3)	24.000	24.000	11.000	10.000	22.000	21.000
CAI (μg/m^3)	59.000	56.000	65.000	37.000	51.000	54.000
AQI Level and Descriptor	A, Good	B, Moderate	B, Moderate	A, Good	B, Moderate	B, Moderate
μCAI (μg/m^3)	53.667					
Overall AQI Level and Descriptor	B, Moderate					

Table 14. AQI of Austrian regions of DO data collection, 2023 (WAQI, 2008)

River	Donau River					
Date of sample collection	September 12	September 7	August 27	August 25	September 2	September 9
Location	Korneuburg	Kloster-neuburg	Donaustadt	Leopoldstadt	Orth an der Donau	Haslau-Maria Ellend
AQI PM2.5 (μg/m^3)	26.667	35.000	23.000	32.000	21.000	27.667
AQI PM10 (μg/m^3)	8.333	17.000	7.000	1.000	14.000	10.000
CAI (μg/m^3)	26.667	35.000	23.000	32.000	21.000	27.667
AQI Level and Descriptor	A, Good	A, Good	A, Good	A, Good	A, Good	A, Good
μCAI (μg/m^3)	27.556					
Overall AQI Level and Descriptor	A, Good					

Table 15. AQI of South Korean regions of pH and TDS data collection, 2024 (WAQI, 2008)

River	Han River					
Date of sample collection	Jul. 13	Jul. 15	Jul. 12	Jul. 14	Jun. 30	Jun. 30

Location	Wabu Eup	Cheonhyeon Dong	Gwangjin Gu	Gangnam Gu	Mapo Gu	Yeongdeungpo Gu
AQI PM2.5 ($\mu g/m^3$)	94.000	78.000	76.000	117.000	69.000	72.000
AQI PM10 ($\mu g/m^3$)	53.000	11.000	34.000	30.000	19.000	17.000
CAI ($\mu g/m^3$)	94.000	78.000	76.000	117.000	69.000	72.000
AQI Level and Descriptor	B, Moderate	B, Moderate	B, Moderate	C, Unhealthy	A, Good	A, Good
µCAI ($\mu g/m^3$)	84.333					
Overall AQI Level and Descriptor	B, Moderate					

Table 16. AQI of Austrian regions of pH and TDS data collection, 2024 (WAQI, 2008)

River	Donau River					
Date of sample collection	Aug. 17	Aug. 17	Aug. 17	Aug. 17	Aug. 19	Aug. 19
Location	Korneuburg	Kloster-neuburg	Donaustadt	Leopoldstadt	Orth an der Donau	Haslau-Maria Ellend
AQI PM2.5 ($\mu g/m^3$)	14.000	31.000	28.000	34.000	42.000	14.000
AQI PM10 ($\mu g/m^3$)	6.333	12.000	11.000	12.000	12.000	4.667
CAI ($\mu g/m^3$)	14.000	31.000	28.000	34.000	42.000	14.000
AQI Level and Descriptor	A, Good	A, Good	A, Good	A, Good	A, Good	A, Good
µCAI ($\mu g/m^3$)	27.167					
Overall AQI Level and Descriptor	A, Good					

When interpreting the AQI data collected, unlike HPD, the CAI values revealed a general trend throughout the regions of the data collection sites instead of appearing to be significantly higher

within the capitals. For instance, Wabu-Eup and Cheonhyeon Dong displayed higher CAI values between 56.000 and 94.000 μg/m^3 during the data collection dates than Mapo Gu and Yeongdeoungpo Gu, which ranged from 51.000 to 72.000 μg/m^3; the CAI values of Klosterneuburg was extremely inflated as well, 35.000 μg/m^3 in 2023 and 31.000 μg/m^3 in 2024, whereas Donaustadt displayed extremely clean air quality with values of 23.000 and 28.000. Such trends suggest that AQI is not directly associated with urbanized areas of population. However, this trend may be limited to the examination of small-scale areas, since the average CAI values of South Korean regions assessed the atmospheric condition as 'B, Moderate' and Austrian regions, which are less populated and industrialized than South Korea, as 'A, Good'. Such overall results further support the possibility of the Han River being of a substandard level of industrial pollution in comparison to Donau River as more pollutants from industries are released into the air.

3.6 Relationship between physicochemical parameters

The data of the selected physicochemical parameters were utilized to reveal a bivariate correlation between each of the variables. Using the Pearson product-moment correlation coefficient, a correlation matrix of the mean physicochemical parameters of each river are presented in Tables 17 and 18. For HPD and AQI, the two datasets from 2023 and 2024 were averaged to be used for calculating the Pearson coefficients.

Table 17. Pearson product-moment correlation coefficient matrix of physicochemical parameters of Han river

	DO	pH	TDS	HPD	AQI
DO	1.000	0.802	-0.527	-0.907	0.527
pH	-	1.000	-0.182	-0.858	0.683
TDS	-	-	1.000	0.188	-0.616
HPD	-	-	-	1.000	-0.432
AQI	-	-	-	-	1.000

Table 18. Pearson product-moment correlation coefficient matrix of physicochemical parameters of Donau river

	DO	pH	TDS	HPD	AQI
DO	1.000	-0.864	0.210	0.254	0.255
pH	-	1.000	-0.607	0.084	-0.317
TDS	-	-	1.000	-0.127	0.239
HPD	-	-	-	1.000	0.299

AQI	-	-	-	-	1.000

A general rule of thumb when interpreting Pearson correlation coefficients is the correlation being considered as strong when the magnitude of the coefficient is larger than 0.5, yet the correlation matrices appear to showcase no common relationships. While DO and pH has a high Pearson coefficient of 0.802 in the Han River, the pair of parameters display a negative trend with a coefficient of -0.858. Additionally, a strong correlation within a river is seemingly weak for the other: while pairs such as DO and HPD or pH and HPD showed extremely strong negative relationships of -0.907 and -0.858, the trends were not apparent from the parameters of the Donau River with coefficients of 0.254 and 0.084 for the respective pairs. Likewise, a moderately high coefficient of 0.527 between DO and AQI of the Donau River was opposed by a low coefficient of 0.255 of the same pair of parameters from the Han River. Hence, the two correlation matrices present the comparison between different sites of the identical river through the given parameters as possible yet imprecise.

To provide an overview of the relationship between the parameters in general, an alternate correlation matrix has been presented in Table 19, cumulatively using the mean of the collected data throughout both rivers.

Table 19. Pearson product-moment correlation coefficient matrix of physicochemical parameters of both rivers

	DO	pH	TDS	HPD	AQI
DO	1.000	0.901	0.892	-0.725	-0.864
pH	-	1.000	0.903	-0.729	-0.918
TDS	-	-	1.000	-0.598	-0.933
HPD	-	-	-	1.000	0.562
AQI	-	-	-	-	1.000

Unlike the previous correlation matrices, Table 19 exhibits high Pearson correlation coefficients between all pairs of physicochemical parameters exploited, ranging from 0.691 to 0.896 in magnitude. Notable pairs of parameters demonstrating extremely strong relationships with each other are DO and pH with a coefficient of 0.901, DO and TDS with a coefficient of 0.8942, pH and AQI with a correlation of -0.918, and AQI and TDS with a correlation of -0.933. However, as the magnitude of the coefficient values are all above 0.562, all correlation between the parameters can be considered as strong. This difference in the strength of the correlation from the previous correlation matrices examining the parameters of each individual river signifies that the zero order relationships between parameters are strongly apparent when considering the correlation from a larger scale, specifically by cumulatively observing rivers instead of scrutinizing the changes between nearby data sites of each body of water.

The trends also align with the assumption of HPD and AQI serving as indicators of industrial pollution, and that they directly correlate with water parameters of nearby rivers. As DO, pH, and TDS displayed a negative Pearson correlation coefficient with the two indicators, all river parameters are inversely related to industrial pollution, with higher values of river parameters signifying lower levels of industrial pollution as well as higher water quality and vice versa. Consequently, all other pairs of parameters display positive relationships. Since all parameters had concluded the Han River's high level of contamination relative to the Donau River, the strong relation between all parameters displayed through the Pearson correlation matrix displays this conclusion as highly reliable. This conclusion also aligns with the trend of the Han River seemingly experiencing greater industrial activities than the Donau River, proposing industrialization as a primary variable affecting the two rivers' water quality and level of pollution. Lastly, the correlation matrix provides all five parameters examined as appropriate for comparing the level of industrial pollution among different rivers.

3.7 Machine-learning modelling of collected data

While the relationship between the five parameters (DO, pH, TDS, HPD, AQI) has been identified, the paper's objective of providing individuals an accessible and affordable method of measuring industrial pollution remains unattained. DO, pH and TDS data can be collected from cheap meters with acceptable margin of error, while HPD is frequently calculated by the government with nearly perfect accuracy; however, AQI is a value that is limited in public data due to the low number of data collection centers yet requires advanced tools costing up to thousands of dollars to accurately measure air pollution, resulting in data being low in accuracy and even inaccessible in some areas.

Hence, to resolve this issue while also exemplifying the possibility of applying the paper's finding about the parameters, various computerized models estimating AQI based on data of other parameters were created. Since individuals would be using such models to estimate AQI for a specific river, the data set was split into the data of the Han and the Donau River, using the first set to train the model and second set to compare the predictions and actual values. As the study researched for AQI and HPD of years 2023 and 2024 since the river parameters were collected during both years, the mean AQI and HPD values were utilized as the testing set. The built-in standard scaler within the library was utilized to allow the variables to be calibrated and balanced by the models.

3.8 Accuracy of the models

In addition to the five base models and the three feature selection methods/dimensionality reduction techniques mentioned in the methodology, up to two layers of feature selection were applied to create the models. Models in which four or more features are selected were removed because feature selection is intended to narrow down the total number of parameters used to predict AQI (CAI was once again selected as the type of AQI for predictions). For a similar reason, 2-layer models in which the second layer selects the same number of features as the first layer or more were not considered as well. Since little to no prior research of modelling these parameters had been conducted for these parameters, combinations of feature selection

methods (PCA, RFE, UNI) and base regressors/classifiers (Linear, SLP, Lasso, Linear SVR, RFR) mentioned above were tested, resulting in a total of 185 models. The results for all models are given in the Appendix. The paper tests various computerized models, using Root Mean Squared Error (RMSE) and mean absolute error (MAE) between the predicted values and actual values of AQI to evaluate its accuracy. The mean, maximum, minimum and second smallest RMSEs as well as MAEs of the tested models are displayed in Tables 20 and 21.

Table 20. Mean, minimum and maximum RMSE of tested models

	Base model	1st feature selection layer	Number of features selected	2nd feature selection layer	Number of features selected	RMSE
Mean	-	-	-	-	-	49.806
Maximum	Linear Regression	PCA	3	RFE, UNI	2	79.902
Minimum	Lasso Regression	-	-	-	-	30.324
Second Smallest	Linear	-	-	-	-	30.542

Table 21. Mean, minimum and maximum MAE of tested models

	Base model	1st feature selection layer	Number of features selected	2nd feature selection layer	Number of features selected	MAE
Mean	-	-	-	-	-	49.131
Maximum	Linear Regression	PCA	3	RFE, UNI	2	78.433
Minimum	Lasso Regression	-	-	-	-	26.014
Second Smallest	Linear Regression	-	-	-	-	26.206

Generally, the RMSE and MAE of all models were generally quite high. The RMSE ranged significantly from 30.324 (Lasso Regression) to 79.902 (Linear-PCA3-RFE2 and Linear-PCA3-UNI2 models); the MAE varied within a similar range from 26.014 (Lasso Regression) to 78.433 (Linear-PCA3-RFE2 and Linear-PCA3-UNI2 models). Based on both errors, the Lasso Regression model without any feature selection layers appears to be the most accurate. The RMSE of the predictions using Lasso Regression was 30.324, slightly smaller

than that of Linear Regression, 30.542. Likewise, its MAE of 26.014 was similar to that of the Linear Regression of 26.206. Lasso Regression's MAE was 61% of the mean MAE of 49.806 and the rMSE was 53% of mean rMSE 49.131, showing the significant accuracy of its programs compared to other models. Hence, although the models seem inaccurate and insignificant for estimating AQI using the four parameters, the SVR-PCA2-RFE1 model can be considered as providing AQI predictions that are of acceptable accuracy. Through this model, the level of industrial pollution within an area will be able to be tested affordably, raising interest for the impacts of industrial pollution and ultimately motivating individuals to advocate against this destruction of the environment.

3.9 Identifying cause of inaccurate predictions

The large errors of the models' predictions were expected due to a number of limitations regarding the parameters and data. Firstly, AQI itself is a very volatile parameter since there is an extensive number of fast-changing uncontrolled variables affecting it, such as strength of wind, rate at which pollutants are released into the air or type of weather; in conjunction with the restrictive amount of AQI collection sites and data available, the inaccuracy within the data set complicates the process of predicting AQI data. Another possible reason is the smaller number of data collection sites themselves, as 12 sites signifying 6 data points used for training and 6 for testing the model, which is an extremely small amount. Likewise, the limited number of parameters presumably restricted the number of patterns the model was able to identify, increasing its inexactness. However, the most influential factor causing the imprecision of the models is likely the clustering of data based on rivers, since the paper has already identified that the river data is clustered together and hence requires data from more rivers (collected with the same methodology) to accurately model the general relationship between the parameters and industrial pollution throughout rivers. As data is clustered, datasets from more than one river are required to form a semi-accurate regression that identifies the trends throughout each river instead of being specific to one river. This major limitation can be resolved through a machine-learning approach where online databases of data can be implemented to the computerized models, which would significantly increase its accuracy. The clustering is demonstrated within the scatterplots provided in Figure 2, in which the plots to the left are based on data from the Han River and plots to the right are of the Donau River.

Figure 2. Scatterplots of each parameter against AQI demonstrating clustering of data (Han river dataset in blue, Donau river dataset in orange)

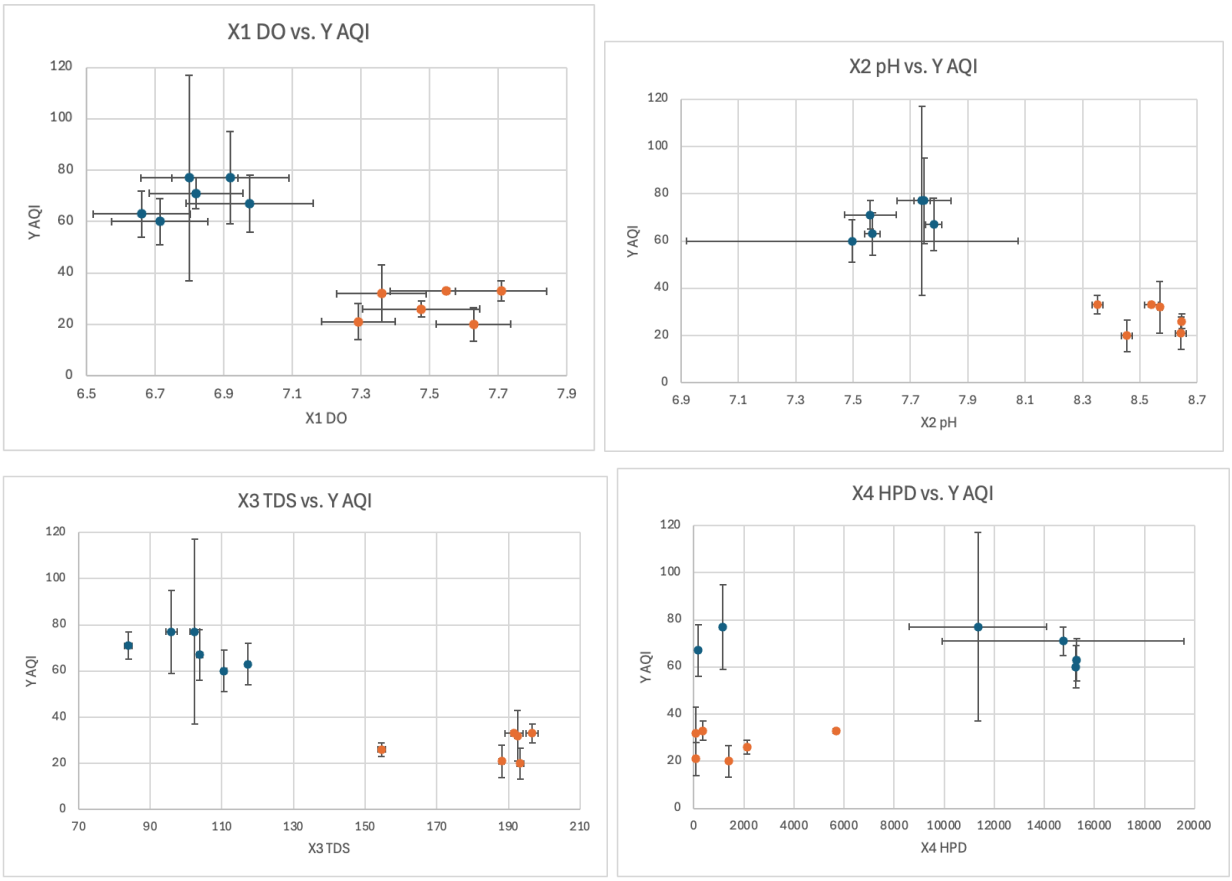

3.10 Analyzing possibility of improving the model

To consider whether an increased number of rivers within the dataset has a possibility of improving the model's predictions of the AQIs, the clustering must be present throughout the analysis of the model, allowing the model to create a regression passing through every cluster. While analyzing the clustering of data for every model would be ideal, creating and examining scatterplots of 185 combinations of models and feature selections would prolong and complicate the study to a great extent. Hence, the scatterplots of data after normalization and applying PCA feature selection were selected for analysis as such scatterplots are apt for visualization. The scatterplot of initial data is provided alongside that of normalized data in Figure 3.

Figure 3. Scatterplots of initial and normalized data

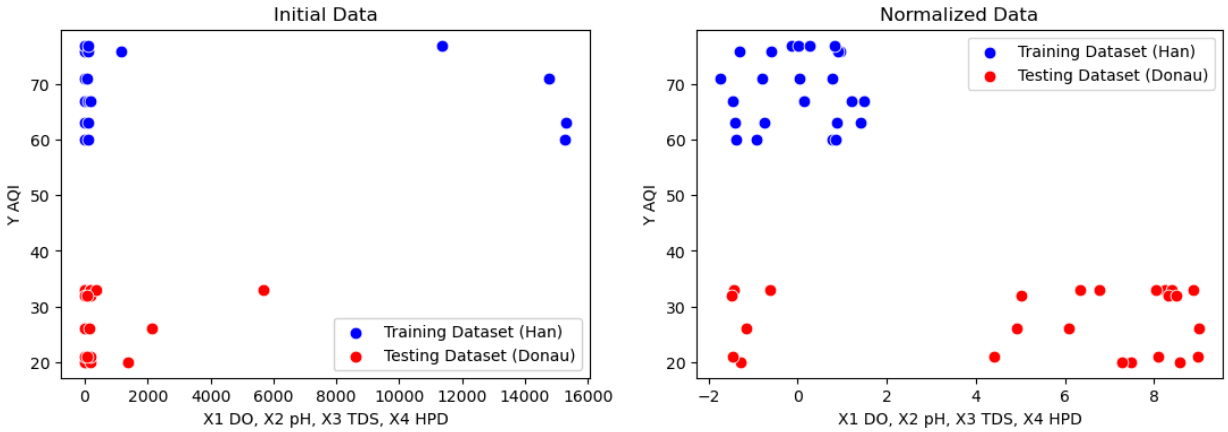

As demonstrated by the clear difference in the plots shown in Figure 3, the clustering of the data from the Han and Donau river appears more evident: while four outliers from the training dataset (Han river) dataset were initially located in the upper right-hand corner, the outliers became part of the cluster after normalizing the data. Contrastingly, new outliers appeared among the testing dataset (Donau river) although of a less extreme degree than the previous outliers, suggesting the limitations of clustering of data with only normalization. For a more detailed analysis of the outliers, scatterplots labelled with specific parameters are provided in Figure 4.

Figure 4. Labelled scatterplots of initial and normalized data

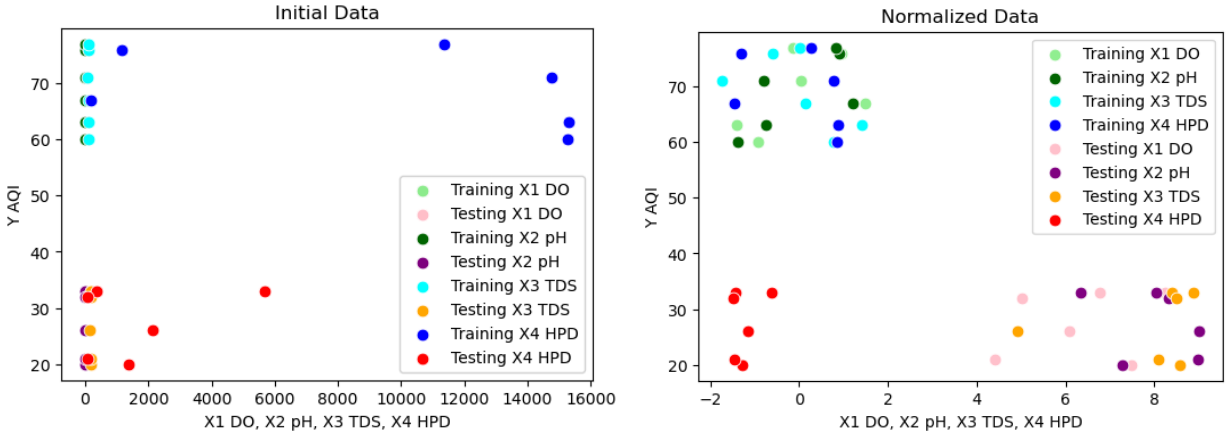

As noticeable through the plots in Figure 4, the outliers from both rivers were due to HPD data from both rivers. This observation suggests that models of greater datasets can predict AQI with a relatively high accuracy if feature selection layers were applied and effectively removed HPD data. However, this is based on the assumption that HPD data of all rivers does not complement the overall trend of the dataset in comparison to DO, pH and HPD, which cannot be justified with data from only two rivers. Subsequently, the scatterplots after applying PCA were analyzed to investigate if HPD data was removed from the testing and training dataset.

Figure 5. Scatterplots of normalized data after applying PCA

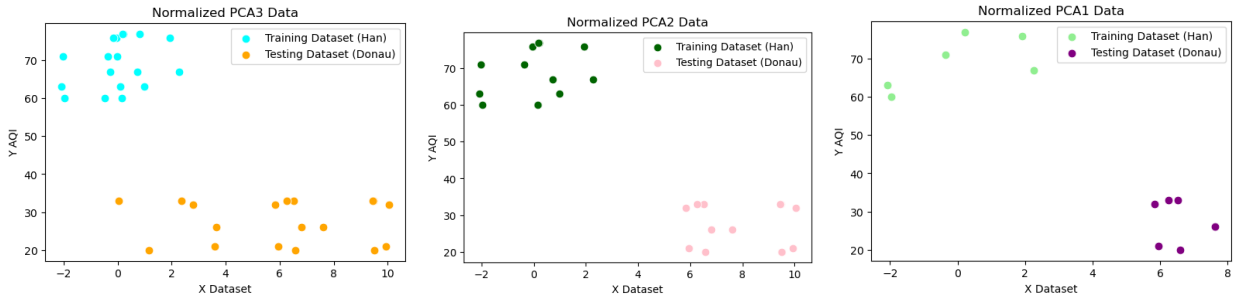

After PCA was applied, the assumption of HPD being removed from the dataset was proven true, further justifying the possibility for the machine-learning model being able to predict AQI more accurately with greater datasets: comparing with scatterplot of the normalized data, the outliers were removed after applying PCA of 3, 2 and 1 components. The clustering is most prominently evident in PCA2, leading to the prediction that selecting two features would provide the most accurate model after more data is added.

3.11 Model with increased dataset

After identifying that the inaccuracy of the model was likely due to the clustering of data public data was utilized to increase the dataset of rivers the model could be trained and tested with [16-19]. Two different sets of data were tested: 2015-2024 and 2019-2024, each of 65 and 44 rivers from various nations around the world. Similar to the scatterplots above, DO, pH, TDS and HPD were used as variables X1 to X4 to predict the Y variable, AQI. Additionally, because total population appeared to show correlation with the predictions when testing, additional datasets of population were considered as the X5 variable. Using the mean values and considering each river as a plot, the dataset was shuffled with the models to test the model's reliability by randomizing the large number of data it uses for training and testing. All models (regressors and classifiers) discussed above were utilized and dimensionality reduction techniques were distinguished from feature selection methods and applied as the last layer of the model to ensure accuracy by undergoing noise reduction with feature selection before changing interpretability with dimensionality reduction; this procedure allowed 11,632 different permutations to be tested, accumulating to be over 45,000 for all datasets combined. RFE was not applied to NuSVR, Epsilon SVR, BR or HGBR because such regressors do not rank features automatically, which is required to implement RFE. K fold Cross-Validation was also implemented to increase accuracy of model, and 5 folds were conducted for each permutation. As the data was randomized, five trials were conducted to confirm its accuracy. The results of the minimum errors are provided in Tables 22 to 33.

Table 22. Mean and Standard Deviation RMSE and MAE of X1-X4 variables for 2015-2024 dataset linear models

2015-2024 X1-X4 Linear Model Mean Error									
	Base model	Feature Selection Method	Parameters Kept	Dimensionality Reduction Technique	Parameters Kept	CV MSE	CV MAE	Final MSE	Final MAE
Overall Mean	-	-	-	-	-	1999.811	19.264	3081.860	22.485
Minimum CV-Final MSE Difference	Elastic Net	CHISQ	3	KPCA-3	2	659.144	19.991	652.036	20.805

Minimum CV-Final MAE Difference	LR	None	4	KPCA-5	2	1874.194	17.325	775.377	17.328
Minimum Final MSE	SLP	None	4	LPCA	2	450.164	10.927	46.769	3.077
Minimum Final MAE	SLP	None	4	LPCA	2	450.164	10.927	46.769	3.077

Table 23. Mean and Standard Deviation RMSE and MAE of X1-X5 variables for 2015-2024 dataset linear models

2015-2024 X1-X5 Linear Model Mean Error									
	Base model	Feature Selection Method	Parameters Kept	Dimensionality Reduction Technique	Parameters Kept	CV MSE	CV MAE	Final MSE	Final MAE
Overall Mean	-	-	-	-	-	6992.036	15.889	5943.822	17.129
Minimum CV-Final MSE Difference	Elastic Net	None	4	TSVD	3	479.060	17.327	479.093	18.491
Minimum CV-Final MAE Difference	Elastic Net	None	4	KPCA-6	2	444.135	15.526	296.098	15.511
Minimum Final MSE	SLP	None	4	None	4	102.922	5.867	46.769	3.077
Minimum Final MAE	SLP	None	4	None	4	102.922	5.867	46.769	3.077

Table 24. Mean and Standard Deviation RMSE and MAE of X1-X4 variables for 2019-2024 dataset linear models

2019-2024 X1-X4 Linear Model Mean Error									
	Base model	Feature Selection Method	Parameters Kept	Dimensionality Reduction Technique	Parameters Kept	CV MSE	CV MAE	Final MSE	Final MAE
Overall Mean	-	-	-	-	-	279639.413	40.974	7731.088	27.229
Minimum CV-Final MSE Difference	Lasso	ANOVA	3	KPCA-C	1	601.621	19.463	601.957	21.098
Minimum CV-Final MAE Difference	LR	None	4	KPCA-R	3	662.638	19.800	581.299	19.802
Minimum Final MSE	Logistic	ANOVA	3	ICA	2	523.257	9.600	1.000	0.333
Minimum Final MAE	Logistic	ANOVA	3	ICA	2	523.257	9.600	1.000	0.333

Table 25. Mean and Standard Deviation RMSE and MAE of X1-X5 variables for 2019-2024 dataset linear models

2019-2024 X1-X5 Linear Model Mean Error

	Base model	Feature Selection Method	Parameters Kept	Dimensionality Reduction Technique	Parameters Kept	CV MSE	CV MAE	Final MSE	Final MAE
Overall Mean	-	-	-	-	-	36908.307	18.569	12352.085	18.287
Minimum CV-Final MSE Difference	SLP	RFE	3	KPCA-5	2	51.686	4.200	52.111	4.778
Minimum CV-Final MAE Difference	Lasso	RFE	3	KPCA-R	1	194.330	11.284	203.258	11.280
Minimum Final MSE	Logistic	ANOVA	3	KPCA-3	2	48.886	4.200	1.000	0.333
Minimum Final MAE	Logistic	ANOVA	3	KPCA-3	2	48.886	4.200	1.000	0.333

Table 26. Mean and Standard Deviation RMSE and MAE of X1-X4 variables for 2015-2024 dataset SVR models

2015-2024 X1-X4 SVR Model Mean Error									
	Base model	Feature Selection Method	Parameters Kept	Dimensionality Reduction Technique	Parameters Kept	CV MSE	CV MAE	Final MSE	Final MAE
Overall Mean	-	-	-	-	-	3.431E+28	1.459E+12	4.512E+27	8.457E+11
Minimum CV-Final MSE Difference	NSVR-S	ANOVA	3	KPCA-5	1	589.657	19.122	588.772	20.095
Minimum CV-Final MAE Difference	NSVR-S	ANOVA	3	KPCA-S	2	610.172	18.686	556.596	18.686
Minimum Final MSE	NSVR-5	ANOVA	3	None	3	3898691.445	282.063	291.698	13.926
Minimum Final MAE	ESVR-5	CHISQ	3	KPCA-C	2	292.877	11.153	434.897	13.692

Table 27. Mean and Standard Deviation RMSE and MAE of X1-X5 variables for 2015-2024 dataset SVR models

2015-2024 X1-X5 SVR Model Mean Error									
	Base model	Feature Selection Method	Parameters Kept	Dimensionality Reduction Technique	Parameters Kept	CV MSE	CV MAE	Final MSE	Final MAE
Overall Mean	-	-	-	-	-	5.927E+11	3917.508	1.771E+8	640.411
Minimum CV-Final MSE Difference	ESVR-6	ANOVA	2	SPCA	1	145.064	9.607	145.089	9.953
Minimum CV-Final MAE Difference	ESVR-S	None	4	KPCA-S	3	484.694	16.666	425.420	16.666

Minimum Final MSE	ESVR-3	ANOVA	3	FA	2	132.039	8.746	111.600	8.368
Minimum Final MAE	ESVR-5	ANOVA	2	ICA	2	335.152	11.974	120.793	8.072

Table 28. Mean and Standard Deviation RMSE and MAE of X1-X4 variables for 2019-2024 dataset SVR models

2019-2024 X1-X4 SVR Model Mean Error									
	Base model	Feature Selection Method	Parameters Kept	Dimensionality Reduction Technique	Parameters Kept	CV MSE	CV MAE	Final MSE	Final MAE
Overall Mean	-	-	-	-	-	5.922E+36	1.238E+16	4.275E+30	3.503E+13
Minimum CV-Final MSE Difference	ESVR-2	ANOVA	3	TSVD	1	1362.7440	20.546	1358.390	15.779
Minimum CV-Final MAE Difference	NSVR-4	ANOVA	2	KPCA-3	1	1861.694	35.086	1273.555	35.065
Minimum Final MSE	NSVR-5	ANOVA	3	None	3	57573160.313	1300.346	66.922	6.793
Minimum Final MAE	ESVR-4	ANOVA	3	TSVD	2	748920.486	165.124	73.080	5.600

Table 29. Mean and Standard Deviation RMSE and MAE of X1-X5 variables for 2019-2024 dataset SVR models

2019-2024 X1-X5 SVR Model Mean Error									
	Base model	Feature Selection Method	Parameters Kept	Dimensionality Reduction Technique	Parameters Kept	CV MSE	CV MAE	Final MSE	Final MAE
Overall Mean	-	-	-	-	-	3.144E+30	6.402E+12	4.558E+8	1723.776
Minimum CV-Final MSE Difference	NSVR-3	CHISQ	2	TSVD	1	59.547	6.917	58.557	7.122
Minimum CV-Final MAE Difference	ESVR-2	ANOVA	2	FA	1	806.276	18.866	728.487	18.865
Minimum Final MSE	ESVR-6	ANOVA	2	ICA	2	1003.620	13.230	0.895	0.403
Minimum Final MAE	ESVR-6	ANOVA	2	ICA	2	1003.620	13.230	0.895	0.403

Table 30. Mean and Standard Deviation RMSE and MAE of X1-X4 variables for 2015-2024 dataset model ensembles

2015-2024 X1-X4 Model Ensemble Mean Error

	Base model	Feature Selection Method	Parameters Kept	Dimensionality Reduction Technique	Parameters Kept	CV MSE	CV MAE	Final MSE	Final MAE
Overall Mean	-	-	-	-	-	251.360	8.044	346.809	9.905
Minimum CV-Final MSE Difference	ETR-S	ANOVA	2	ICA	1	77.075	3.971	77.087	4.163
Minimum CV-Final MAE Difference	ABR-S	PCR	3	KPCA-5	1	93.362	6.795	146.884	6.795
Minimum Final MSE	GBR-HS	CHISQ	3	KPCA-S	2	204.218	6.334	36.968	3.646
Minimum Final MAE	ETR-F	ANOVA	3	SPCA	1	41.388	1.945	48.849	1.938

Table 31. Mean and Standard Deviation RMSE and MAE of X1-X5 variables for 2015-2024 dataset model ensembles

2015-2024 X1-X5 Model Ensemble Mean Error									
	Base model	Feature Selection Method	Parameters Kept	Dimensionality Reduction Technique	Parameters Kept	CV MSE	CV MAE	Final MSE	Final MAE
Overall Mean	-	-	-	-	-	165.866	5.889	218.801	6.758
Minimum CV-Final MSE Difference	ABR-E	ANOVA	3	LPCA	2	52.863	3.719	52.868	2.946
Minimum CV-Final MAE Difference	RFR-F	MIT	3	KPCA-3	1	55.847	2.853	63.397	2.852
Minimum Final MSE	GBR-SF	PCR	3	KPCA-C	2	437.481	9.931	36.623	3.191
Minimum Final MAE	GBR-HF	PCR	2	ICA	2	23.093	1.343	41.463	1.786

Table 32. Mean and Standard Deviation RMSE and MAE of X1-X4 variables for 2019-2024 dataset model ensembles

2019-2024 X1-X4 Model Ensemble Mean Error									
	Base model	Feature Selection Method	Parameters Kept	Dimensionality Reduction Technique	Parameters Kept	CV MSE	CV MAE	Final MSE	Final MAE
Overall Mean	-	-	-	-	-	489.455	11.244	404.154	7.831
Minimum CV-Final MSE Difference	RFR-F	ANOVA	3	KPCA-2	2	422.365	9.954	423.193	8.943
Minimum CV-Final MAE Difference	BR	CHISQ	3	KPCA-C	2	606.700	14.254	630.299	14.256
Minimum Final MSE	GBR-HF	ANOVA	1	None	1	321.715	6.869	4.052E-6	1.599E-3

Minimum Final MAE	GBR-HF	ANOVA	1	None	1	321.715	6.869	4.052E-6	1.599E-3

Table 33. Mean and Standard Deviation RMSE and MAE of X1-X5 variables for 2019-2024 dataset model ensembles

2019-2024 X1-X5 Model Ensemble Mean Error									
	Base model	Feature Selection Method	Parameters Kept	Dimensionality Reduction Technique	Parameters Kept	CV MSE	CV MAE	Final MSE	Final MAE
Overall Mean	-	-	-	-	-	187.364	6.362	117.405	3.017
Minimum CV-Final MSE Difference	GBR-AF	RFE	2	None	2	12.162	1.539	11.678	2.057
Minimum CV-Final MAE Difference	RFR-F	RFE	2	KPCA-6	1	26.342	2.581	16.559	9.783
Minimum Final MSE	GBR-AF	ANOVA	1	None	1	11.962	1.405	1.672E-6	8.736E-4
Minimum Final MAE	GBR-AF	ANOVA	1	None	1	11.962	1.405	1.672E-6	8.736E-4

The low values of mean error clearly indicates that the models using the large datasets demonstrated a significant degree of accuracy. Furthermore, NSVR-3 with CHISQ2 and TSVD1 or RFR-F with RFE2 and KPCA1-6 exemplify models of minimal difference between average cross validation error and final error after testing, showing that models have not been overfitted and are reliable. While nonlinear SVRs appear to be the most accurate with minimum MSE and MAE of 0.895 and 0.403, different models displayed above can be selected based on the objective of the user, such as minimizing CV-Final error difference or prioritizing MAE over MSE.

4. Limitations

4.1 Limitations of data collection

A notable limitation of the case study is the considerable variation observed between data points. The fluctuations in environmental variables, such as sample temperature, were more pronounced in situ due to the volatile conditions present at the site. In contrast, the physical data concerning dissolved oxygen exhibited significant discrepancies when compared to the pH and TDS data, likely as a result of the data being collected ex-situ. Additionally, the differing midstream data collection sites in 2023 and 2024, while accounting for the distance between locations to a certain extent, led to variations in the population density values for that section.

4.2 Limitations of data modelling

The finding of feature selection increasing the accuracy of the machine-learning models is contradictory to the most accurate model trained with Han and Donau River being Lasso regression trained using normalized data without feature selection layers. However, this counterclaim can be easily resolved since all models showcased high degrees of errors and the selected model is still inaccurate nonetheless.

5. Conclusion

This study aimed to examine the industrial pollution among the Han River of South Korea and the Donau RIver of Austria, collecting data on DO, pH and TDS as parameters of the rivers' surface water. The study also correlated various parameters to explore relationships and identify reliable indicators, using the Pearson's Correlation Coefficient matrices to interconnect the physically collected data alongside public data of HPD and AQI used as additional parameters. Qualitative evaluation of the severity of industrial pollution among both rivers was conducted as well by identifying variables such as the amount of sewage from factories being discharged into the rivers or consequences of urbanization, which revealed the significant degree at which industrial pollution occurs in South Korea that affects the Han River in comparison to Austria and the Donau River. The data of river parameters, HPD and AQI all aligned with general trends of the Han River being significantly more polluted than the Donau River through data sites demonstrating comparatively high DO and TDS values, low pH values, high HPD values and high AQI values (CAI used as type of AQI), aligning with the qualitative assessment. The correlation matrices showcased asymmetrical patterns when parameters from data sites within the river were compared. However, when compared cumulatively, all pairs of parameters displayed strong zero order relationships with the magnitude of the Pearson coefficient ranging from 0.691 to 0.903. The results present the interconnected relationship between the five parameters examined and the viability of them as indicators of industrial pollution when comparing multiple rivers. The data analysis models created based on such relationships identified between parameters allow for predictions of AQI data with varying accuracy. This ability to predict AQI removes the need for expensive measurement devices for identifying the level of industrial pollution, allowing for the general audience to access or obtain such data and raising awareness for the global issue of climate change. Similarly, other researchers can utilize the model(s) to estimate AQI based on other interconnected parameters, broadening their scope of research. The study affirms that the Han River as experiencing severe industrial pollution whereas the Donau River is being contaminated to a tolerable degree, supported by the collected data of physicochemical parameters from the rivers' surface water, HPD and AQI values of the data sites, and the multitude of factors affecting the rivers' industrial pollution. The study also establishes Lasso Regression models as appropriate for predicting AQI as AQI with some errors, the RMSE and MAE being comparatively low values of 30.324 and 26.014, respectively. In the near future, implementing a machine-learning approach using databases of data is also possible, allowing for improvement in its accuracy as well as possibly suggesting different models to be more suitable for predictions. Lastly, ESVR-6 applying ANOVA2 and ICA2

appears to be the most accurate model with final MSE and MAE of 0.895 and 0.403, but as models such as NSVR-3 with CHISQ2 and TSVD1 or RFR-F with RFE2 and KPCA1-6 showcase smaller difference between average Cross-Validation and final error, different models can be selected for different purposes with the majority of models ensuring high accuracy in all categories nonetheless.

CRediT authorship contribution statement

Jiwoo Jung: Conceptualization, Data curation, Formal analysis, investigation, Methodology, Resources, Software, Validation, Visualization, Writing – original draft, Writing – review & editing. **Leon Plakolm:** Project administration, Supervision, Validation, Writing – review & editing.

Acknowledgements

I would like to acknowledge Ms. Rosalie Rozema for encouraging me to further advance this research project.

Data Availability

Data and code are publicly available on Github depositories.

Han-Donau Model Github Repository: https://github.com/jiwj07/Han_Donau_Data_Models
2015-2024 Model Github Repository: https://github.com/jiwj07/2015_2024_Data_Models
2019-2024 Model Github Repository: https://github.com/jiwj07/2019_2024_Data_Models
Linear Models X1-X4 2015-2024 Github Repository: https://github.com/jiwj07/2015_2024_X1_X4_Linear_Models
Linear Models X1-X4 2019-2024 Github Repository: https://github.com/jiwj07/2019_2024_X1_X4_Linear_Models
Linear Models X1-X5 2015-2024 Github Repository: https://github.com/jiwj07/2015_2024_X1_X5_Linear_Models
Linear Models X1-X5 2019-2024 Github Repository: https://github.com/jiwj07/2019_2024_X1_X5_Linear_Models
SVR Models X1-X4 2015-2024 Github Repository: https://github.com/jiwj07/2015_2024_X1_X4_SVR_Models
SVR Models X1-X4 2019-2024 Github Repository: https://github.com/jiwj07/2019_2024_X1_X4_SVR_Models
SVR Models X1-X5 2015-2024 Github Repository: https://github.com/jiwj07/2015_2024_X1_X5_SVR_Models
SVR Models X1-X5 2019-2024 Github Repository: https://github.com/jiwj07/2019_2024_X1_X5_SVR_Models
Model Ensembles X1-X4 2015-2024 Github Repository: https://github.com/jiwj07/2015_2024_X1_X4_Model_Ensembles
Model Ensembles X1-X4 2019-2024 Github Repository: https://github.com/jiwj07/2019_2024_X1_X4_Model_Ensembles
Model Ensembles X1-X5 2015-2024 Github Repository: https://github.com/jiwj07/2015_2024_X1_X5_Model_Ensembles
Model Ensembles X1-X5 2019-2024 Github Repository: https://github.com/jiwj07/2019_2024_X1_X5_Model_Ensembles

References

Acar, S., & Mahmut Tekce. (2014). Economic Development and Industrial Pollution in the Mediterranean Region: A Panel Data Analysis. Retrieved December 9, 2024, from Loyola eCommons website: https://ecommons.luc.edu/meea/190/

AirKorea: Introduction to the AQI. (2022). Retrieved December 10, 2024, from Airkorea.or.kr website: https://www.airkorea.or.kr/eng/khaiInfo?pMENU_NO=166

An, I. (2022, September 15). Breaking News/ 11 Million Tons of Polluted Sewage Discharged into Han River Basin/Day, “Pollution of Drinking Water Sources Worsened.” Retrieved December 16, 2024, from Egreen News website: https://m.egreen-news.com/11480

Anderson, E. P., Jackson, S., Tharme, R. E., Douglas, M., Flotemersch, J. E., Zwarteveen, M., … Roux, D. J. (2019). Understanding rivers and their social relations: A critical step to advance environmental water management. *WIREs Water*, *6*(6). https://doi.org/10.1002/wat2.1381

Andrej Dávid, & Madudová, E. (2019). The Danube river and its importance on the Danube countries in cargo transport. *Transportation Research Procedia*, *40*, 1010–1016. https://doi.org/10.1016/j.trpro.2019.07.141

Anh, N. T., Can, L. D., Nhan, N. T., Schmalz, B., & Luu, T. L. (2023). Influences of key factors on river water quality in urban and rural areas: A review. *Case Studies in Chemical and Environmental Engineering*, *8*, 100424. https://doi.org/10.1016/j.cscee.2023.100424

Arief Dhany Sutadian, Nitin Muttil, Yilmaz, A. G., & Perera, C. (2015). Development of river water quality indices—a review. *Environmental Monitoring and Assessment*, *188*(1). https://doi.org/10.1007/s10661-015-5050-0

Bashir, I., Lone, F. A., Bhat, R. A., Mir, S. A., Dar, Z. A., & Dar, S. A. (2020). Concerns and Threats of Contamination on Aquatic Ecosystems. *Springer EBooks*, 1–26. https://doi.org/10.1007/978-3-030-35691-0_1

Bhuyan, M. S., & Islam, M. S. (2017). Status and Impacts of Industrial Pollution on the Karnafully River in Bangladesh: A Review. *International Journal of Marine Science*. https://doi.org/10.5376/ijms.2017.07.0016

Blanchet, S., Prunier, J. G., Paz-Vinas, I., Keoni Saint-Pé, Rey, O., Raffard, A., … Dubut, V. (2020). A river runs through it: The causes, consequences, and management of intraspecific diversity in river networks. *Evolutionary Applications*, *13*(6), 1195–1213. https://doi.org/10.1111/eva.12941

Cho, C. (2023, June 15). The Han River has the 43rd highest contamination density in the world. Retrieved December 16, 2024, from The Herald Insight website: http://www.heraldinsight.co.kr/news/articleView.html?idxno=3205#:~:text=According%20to%20research%2C%20the%20Han,filtered%20by%20wastewater%20treatment%20plants.

Die Donaustadt in Zahlen - Statistiken zum 22. Bezirk. (2020, December 15). Retrieved December 10, 2024, from Wien.gv.at website: https://www.wien.gv.at/statistik/bezirke/donaustadt.html

Die Leopoldstadt in Zahlen - Statistiken zum 2. Bezirk. (2020, December 14). Retrieved December 10, 2024, from Wien.gv.at website: https://www.wien.gv.at/statistik/bezirke/leopoldstadt.html

Ein Blick auf die Gemeinde Korneuburg: 1.1 Fläche und Flächennutzung. (2024, January 1). Retrieved December 10, 2024, from Statistik.at website: https://www.statistik.at/blickgem/G0101/g31213.pdf

Gasparotti, C. M. (2014). The main factors of water pollution in Danube River basin. *Euro Economica*, *33*(01), 91–106. Retrieved from https://www.ceeol.com/search/article-detail?id=284478

Google Maps. (2019). Google Maps. Retrieved December 16, 2024, from Google Maps website: https://www.google.com/maps

Gunkel, G., Kosmol, J., Sobral, M., Rohn, H., Montenegro, S., & Aureliano, J. (2006). Sugar Cane Industry as a Source of Water Pollution – Case Study on the Situation in Ipojuca River, Pernambuco, Brazil. *Water Air & Soil Pollution*, *180*(1-4), 261–269. https://doi.org/10.1007/s11270-006-9268-x

Hanam Province Official E-Government Website. (2023). Neighborhood News - Administrative Welfare Center. Retrieved December 11, 2024, from Hanam.go.kr website: https://www.hanam.go.kr/jumin/contents.do?key=11326

Helmut Habersack, Hein, T., Stanica, A., Liska, I., Mair, R., Jäger, E., … Bradley, C. (2015). Challenges of river basin management: Current status of, and prospects for, the River Danube from a river engineering perspective. *The Science of the Total Environment*, *543*, 828–845. https://doi.org/10.1016/j.scitotenv.2015.10.123

Hwang, J. H., Park, S. H., & Song, C. M. (2020). A Study on an Integrated Water Quantity and Water Quality Evaluation Method for the Implementation of Integrated Water Resource Management Policies in the Republic of Korea. *Water*, *12*(9), 2346–2346. https://doi.org/10.3390/w12092346

International Commission for the Protection of the Danube River. (2021). Water Quality. Retrieved December 16, 2024, from Icpdr.org website: https://www.icpdr.org/tasks-topics/topics/water-quality

International Commission for the Protection of the Danube River. (2022, June 9). Annual Bathing Water Report Published: Danube Countries at Top of Ranking | ICPDR - International Commission for the Protection of the Danube River. Retrieved December 16, 2024, from Icpdr.org website: https://www.icpdr.org/tasks-topics/topics/water-quality/annual-bathing-water-report-published-danube-countries-top

Jung, D. (2019, October 28). Han river water pollution, highest accident rate among the four major rivers. Retrieved December 16, 2024, from Oh My News website: https://www.ohmynews.com/NWS_Web/View/at_pg.aspx?CNTN_CD=A0002582171

Kim, H.-K., & Seoul National University Graduate School of Environmental Studies. (2024). The Modern Evolution of Environmentalism : The Case of Korea, 1960~1989. *Journal of Environmental Studies*, *28*, 30–41. https://hdl.handle.net/10371/90500

Kondolf G. Mathias, & Pinto, P. J. (2016). The social connectivity of urban rivers. *Geomorphology*, *277*, 182–196. https://doi.org/10.1016/j.geomorph.2016.09.028

Lee, S. D., Yun, S. M., Cho, P. Y., Yang, H.-W., & Kim, O. J. (2019). Newly Recorded Species of Diatoms in the Source of Han and Nakdong Rivers, South Korea. *Phytotaxa*, *403*(3), 143–143. https://doi.org/10.11646/phytotaxa.403.3.1

Lin, L., Yang, H., & Xu, X. (2022). Effects of Water Pollution on Human Health and Disease Heterogeneity: A Review. *Frontiers in Environmental Science*, *10*. https://doi.org/10.3389/fenvs.2022.880246

Ministry of the Interior and Safety of South Korea. (2015). Resident Registration Population Statistics Ministry of the Interior and Safety. Retrieved December 11, 2024, from Mois.go.kr website: https://jumin.mois.go.kr/

Mishra, R. K., Mentha, S. S., Misra, Y., & Dwivedi, N. (2023). Emerging pollutants of severe environmental concern in water and wastewater: A comprehensive review on current developments and future research. *Water-Energy Nexus*, *6*, 74–95. https://doi.org/10.1016/j.wen.2023.08.002

Mohamed, A. (2024). *Water Pollution: Causes, Impacts, and Solutions: a critical review*. (76), 1–18. https://doi.org/10.37376/jsh.vi76.5785

Namyangju Province Official E-Government Website. (2024). General information - Introduction - Wabu-eup - Administrative welfare center/town/village - Namyangju introduction - Namyangju City Hall. Retrieved December 11, 2024, from Namyangju City Hall website: https://www.nyj.go.kr/www/contents.do?key=2569

Olías, M., Cerón, J. C., Moral, F., & Ruiz, F. (2006). Water quality of the Guadiamar River after the Aznalcóllar spill (SW Spain). *Chemosphere*, *62*(2), 213–225. https://doi.org/10.1016/j.chemosphere.2005.05.015

P.U Igwe, C.C Chukwudi, F.C Ifenatuorah, I.F Fagbeja, & C.A Okeke. (2017). A Review of Environmental Effects of Surface Water Pollution. *Ijaers.com*, *4*(12). Retrieved from https://ijaers.com/detail/a-review-of-environmental-effects-of-surface-water-pollution/

Radu, V.-M., Ionescu, P., Deak, G., Diacu, E., Ivanov, A. A., Zamfir, S., & Marcus, M.-I. (2020). Overall assessment of surface water quality in the Lower Danube River. *Environmental Monitoring and Assessment*, *192*(2). https://doi.org/10.1007/s10661-020-8086-8

Reinartz, R., Lippold, S., D. Lieckfeldt, & Ludwig, A. (2011). Population genetic analyses of Acipenser ruthenus as a prerequisite for the conservation of the uppermost Danube population. *Journal of Applied Ichthyology*, *27*(2), 477–483. https://doi.org/10.1111/j.1439-0426.2011.01693.x

Research Report - Research on the establishment of a conservation plan for the Han River Estuary Wetland Protection Area (20-24). (2019, October 7). Retrieved December 16, 2024, from Ecopi.co.kr website: http://ecopi.co.kr/index.php?mid=board_NtgR13&document_srl=79524

Roy, M., & Shamim, F. (2020). Research on the Impact of Industrial Pollution on River Ganga: A Review. *International Journal of Prevention and Control of Industrial Pollution*, *6*(1), 43–51. Retrieved from https://chemical.journalspub.info/index.php?journal=JPCIP&page=article&op=view&path%5B%5D=961

Rusydi, A. F. (2018). Correlation between conductivity and total dissolved solid in various type of water: A review. *IOP Conference Series: Earth and Environmental Science*, *118*(1), 012019. https://doi.org/10.1088/1755-1315/118/1/012019

Schmid, M., Haidvogl, G., Friedrich, T., Funk, A., Schmalfuss, L., Schmidt-Kloiber, A., & Hein, T. (2023). The Danube: On the Environmental History, Present, and Future of a Great European River. *UNESCO EBooks*, 637–671. https://doi.org/10.54677/intf8577

Seoul Statistical Integration Platform. (2019). Administrative District Population Statistical Table. Retrieved December 11, 2024, from Eseoul.go.kr website: https://stat.eseoul.go.kr/statHtml/statHtml.do?orgId=201&tblId=DT_201004_O010001&conn_path=I2&obj_var_id=&up_itm_id=

Shin, H.-J., Kim, H., Jeon, C.-H., Jo, M.-W., Nguyen, T., & Tenhunen, J. (2016). Benefit Transfer for Water Management along the Han River in South Korea Using Meta-Regression Analysis. *Water*, *8*(11), 492–492. https://doi.org/10.3390/w8110492

Shin, M.-S., Lee, J.-Y., Kim, B.-C., & Bae, Y.-J. (2011). Long-term variations in water quality in the lower Han River. *Journal of Ecology and Field Biology*, *34*(1), 31–37. https://doi.org/10.5141/jefb.2011.005

Stagl, J., & Hattermann, F. (2015). Impacts of Climate Change on the Hydrological Regime of the Danube River and Its Tributaries Using an Ensemble of Climate Scenarios. *Water*, *7*(11), 6139–6172. https://doi.org/10.3390/w7116139

Statistik Austria. (2024a, January 1). Ein Blick auf die Gemeinde Haslau-Maria Ellend: 1.1 Fläche und Flächennutzung Q. Retrieved December 10, 2024, from Statistik.at website: https://www.statistik.at/blickgem/G0101/g30711.pdf

Statistik Austria. (2024b, January 1). Ein Blick auf die Gemeinde Klosterneuburg: 1.1 Fläche und Flächennutzung Q. Retrieved December 10, 2024, from Statistik.at website: https://www.statistik.at/blickgem/G0101/g32144.pdf

Statistik Austria. (2024c, January 1). Ein Blick auf die Gemeinde Orth an der Donau: 1.1 Fläche und Flächennutzung Q. Retrieved December 10, 2024, from Statistik.at website: https://www.statistik.at/blickgem/G0101/g30844.pdf

Tahershamsi, A., Bakhtiary, A., & Mousavi, A. (2009). Effects of seasonal climate change on Chemical Oxygen Demand (COD) concentration in the Anzali Wetland (Iran). In *18 th World IMACS / MODSIM*. Retrieved from https://citeseerx.ist.psu.edu/document?repid=rep1&type=pdf&doi=e2ad0665600300db2830f048ad9febc501518e24

Vynokurova, S., Yakovliev, M., Voloshkevich, O., Haidash, O., & Demchenko, V. (2023). Biodiversity assessment of the Danube region as a tool for the development of protected areas in the region. *IOP Conference Series: Earth and Environmental Science*, *1254*(1), 012015. https://doi.org/10.1088/1755-1315/1254/1/012015

World Air Quality Index. (2008). Retrieved December 9, 2024, from aqicn.org website: https://aqicn.org/

Wu, Y., Zhang, L., Wang, J., & Mou, Y. (2021). Communicating Air Quality Index Information: Effects of Different Styles on Individuals' Risk Perception and

Precaution Intention. *International Journal of Environmental Research and Public Health*, *18*(19), 10542–10542. https://doi.org/10.3390/ijerph181910542

Zhang, Z. M., Wang, X. Y., Zhang, Y., Nan, Z., & Shen, B. G. (2012). The Over Polluted Water Quality Assessment of Weihe River Based on Kernel Density Estimation. *Procedia Environmental Sciences*, *13*, 1271–1282. https://doi.org/10.1016/j.proenv.2012.01.120

Buitinck, L., Louppe, G., Blondel, M., Pedregosa, Fabian, Mueller, A., Grisel, O., … Ga"el Varoquaux. (2013). API design for machine learning software: experiences from the scikit-learn project. In ECML PKDD Workshop: Languages for Data Mining and Machine Learning (pp. 108–122).

Cairncross, E. K., John, J., & Zunckel, M. (2007). A novel air pollution index based on the relative risk of daily mortality associated with short-term exposure to common air pollutants. *Atmospheric Environment*, *41*(38), 8442–8454. https://doi.org/10.1016/j.atmosenv.2007.07.003

United Nations Environment Programme. (2024, January 9). *GEMStat - The global freshwater quality database*. GEMStat. https://gemstat.org/

International Database. (2025). Census.gov; United States Census Bureau. https://www.census.gov/data-tools/demo/idb/#/dashboard?dashboard_page=country&COUNTRY_YR_ANIM=2025&CCODE_SINGLE=UY&subnat_map_admin=ADM1&CCODE=UY

UNdata. (2024). Un.org; United Nations. https://data.un.org/

Air quality database 2022. (2022). Who.int; World Health Organization. https://www.who.int/data/gho/data/themes/air-pollution/who-air-quality-database/2022

Appendix

Table A.1. Mean Squared Error(MSE), RMSE and MAE values of the machine-learning models using data from the Han and Donau rivers

Base model	1st feature selection layer	Number of features selected	2nd feature selection layer	Number of features selected	MSE	RMSE	MAE
Linear	-	-	-	-	932.833	30.542	26.206
Perceptron	-	-	-	-	1590.500	39.881	39.500
RFR	-	-	-	-	1694.890	41.169	40.800
Lasso	-	-	-	-	919.574	30.324	26.014
SVR	-	-	-	-	1705.912	41.303	40.935
Linear	PCA	1	-	-	3233.561	56.864	56.561
Linear	PCA	2	-	-	1482.418	38.502	37.881
Linear	PCA	3	-	-	3834.467	61.923	59.753
Linear	RFE	1	-	-	5804.771	76.189	75.790
Linear	RFE	2	-	-	5822.514	76.305	75.830
Linear	RFE	3	-	-	1002.260	31.658	26.960
Linear	UNI	1	-	-	5804.771	76.189	75.790
Linear	UNI	2	-	-	2183.650	46.730	45.626
Linear	UNI	3	-	-	1002.260	31.658	26.960
Perceptron	PCA	1	-	-	1590.500	39.881	39.500
Perceptron	PCA	2	-	-	1342.500	36.640	39.500
Perceptron	PCA	3	-	-	1685.167	41.051	36.167
Perceptron	RFE	1	-	-	1590.500	39.881	40.500
Perceptron	RFE	2	-	-	1590.500	39.881	39.500
Perceptron	RFE	3	-	-	1590.500	39.881	39.500
Perceptron	UNI	1	-	-	1590.500	39.881	39.500
Perceptron	UNI	2	-	-	1590.500	39.881	39.500

Perceptron	UNI	3	-	-	1590.500	39.881	39.500
RFR	PCA	1	-	-	1827.162	42.745	42.390
RFR	PCA	2	-	-	1728.514	41.575	41.210
RFR	PCA	3	-	-	1897.033	43.555	43.180
RFR	RFE	1	-	-	1256.650	35.449	35.020
RFR	RFE	2	-	-	1506.346	38.812	38.420
RFR	RFE	3	-	-	1583.111	39.788	39.405
RFR	UNI	1	-	-	1820.386	42.666	42.310
RFR	UNI	2	-	-	1422.286	37.713	37.310
RFR	UNI	3	-	-	1562.190	39.525	39.140
Lasso	PCA	1	-	-	3233.305	56.862	56.559
Lasso	PCA	2	-	-	1482.972	38.509	37.888
Lasso	PCA	3	-	-	3833.520	61.915	59.747
Lasso	RFE	1	-	-	5803.548	76.181	75.782
Lasso	RFE	2	-	-	5821.096	76.296	75.822
Lasso	RFE	3	-	-	1002.747	31.666	26.972
Lasso	UNI	1	-	-	5803.548	76.181	75.782
Lasso	UNI	2	-	-	2183.612	46.729	45.626
Lasso	UNI	3	-	-	1002.747	31.666	26.972
SVR	PCA	1	-	-	1692.061	41.135	40.765
SVR	PCA	2	-	-	1699.896	41.230	40.861
SVR	PCA	3	-	-	1703.900	41.278	40.910
SVR	RFE	1	-	-	1682.112	41.014	40.643
SVR	RFE	2	-	-	1726.821	41.555	41.189
SVR	RFE	3	-	-	1697.059	41.195	40.827
SVR	UNI	1	-	-	1745.169	41.775	41.412
SVR	UNI	2	-	-	1683.041	41.025	40.654
SVR	UNI	3	-	-	1697.051	41.195	40.827
Linear	PCA	2	PCA	1	3233.561	56.864	56.561
Linear	PCA	2	RFE	1	3233.561	56.864	56.561
Linear	PCA	2	UNI	1	3233.561	56.864	56.561
Linear	PCA	3	PCA	1	3233.561	56.864	56.561
Linear	PCA	3	PCA	2	1482.418	38.502	37.881
Linear	PCA	3	RFE	1	4242.019	65.131	63.372
Linear	PCA	3	RFE	2	6384.359	79.902	78.433

Linear	PCA	3	UNI	1	4242.019	65.131	63.372
Linear	PCA	3	UNI	2	6384.359	79.902	78.433
Linear	RFE	2	PCA	1	5146.629	71.740	71.520
Linear	RFE	2	RFE	1	5804.771	76.189	75.790
Linear	RFE	2	UNI	1	5804.771	76.189	75.790
Linear	RFE	3	PCA	1	3509.894	59.244	58.903
Linear	RFE	3	PCA	2	2449.236	49.490	49.024
Linear	RFE	3	RFE	1	5804.771	76.189	75.790
Linear	RFE	3	RFE	2	5822.514	76.305	75.830
Linear	RFE	3	UNI	1	5804.771	76.189	75.790
Linear	RFE	3	UNI	2	2183.650	46.730	45.626
Linear	UNI	2	PCA	1	1855.391	43.074	41.857
Linear	UNI	2	RFE	1	5804.771	76.189	75.790
Linear	UNI	2	UNI	1	5804.771	76.189	75.790
Linear	UNI	3	PCA	1	3509.894	59.244	58.903
Linear	UNI	3	PCA	2	2449.236	49.490	49.024
Linear	UNI	3	RFE	1	5804.771	76.189	75.790
Linear	UNI	3	RFE	2	5822.514	76.305	75.830
Linear	UNI	3	UNI	1	5804.771	76.189	75.790
Linear	UNI	3	UNI	2	2183.650	46.730	45.626
Perceptron	PCA	2	PCA	1	2382.500	48.811	48.500
Perceptron	PCA	2	RFE	1	1290.500	35.924	35.500
Perceptron	PCA	2	UNI	1	2382.500	48.811	48.500
Perceptron	PCA	3	PCA	1	2382.500	48.811	48.500
Perceptron	PCA	3	PCA	2	1590.500	39.881	39.500
Perceptron	PCA	3	RFE	1	2398.500	48.974	48.500
Perceptron	PCA	3	RFE	2	1290.500	35.924	35.500
Perceptron	PCA	3	UNI	1	2398.500	48.974	48.500
Perceptron	PCA	3	UNI	2	2177.167	46.660	46.167
Perceptron	RFE	2	PCA	1	1579.667	39.745	38.000
Perceptron	RFE	2	RFE	1	2480.500	49.805	49.500
Perceptron	RFE	2	UNI	1	2480.500	49.805	49.500
Perceptron	RFE	3	PCA	1	2382.500	48.811	48.500
Perceptron	RFE	3	PCA	2	1342.500	36.640	36.167
Perceptron	RFE	3	RFE	1	2480.500	49.805	49.500
Perceptron	RFE	3	RFE	2	2480.500	49.805	49.500
Perceptron	RFE	3	UNI	1	2480.500	49.805	49.500
Perceptron	RFE	3	UNI	2	2480.500	49.805	49.500

Perceptron	UNI	2	PCA	1	1579.667	39.745	38.000
Perceptron	UNI	2	RFE	1	2480.500	49.805	49.500
Perceptron	UNI	2	UNI	1	2480.500	49.805	49.500
Perceptron	UNI	3	PCA	1	1922.500	43.846	43.500
Perceptron	UNI	3	PCA	2	1495.833	38.676	37.833
Perceptron	UNI	3	RFE	1	2480.500	49.805	49.500
Perceptron	UNI	3	RFE	2	2480.500	49.805	49.500
Perceptron	UNI	3	UNI	1	2480.500	49.805	49.500
Perceptron	UNI	3	UNI	2	2480.500	49.805	49.500
RFR	PCA	2	PCA	1	1831.404	42.795	42.730
RFR	PCA	2	RFE	1	1872.376	43.271	42.780
RFR	PCA	2	UNI	1	1800.976	42.438	42.990
RFR	PCA	3	PCA	1	1837.350	42.864	42.960
RFR	PCA	3	PCA	2	1726.042	41.546	41.550
RFR	PCA	3	RFE	1	1896.490	43.549	42.320
RFR	PCA	3	RFE	2	1717.816	41.447	41.010
RFR	PCA	3	UNI	1	2058.036	45.366	45.288
RFR	PCA	3	UNI	2	2111.114	45.947	45.282
RFR	RFE	2	PCA	1	1489.584	38.595	36.010
RFR	RFE	2	RFE	1	1268.586	35.617	35.220
RFR	RFE	2	UNI	1	1272.108	35.667	35.310
RFR	RFE	3	PCA	1	1843.306	42.934	43.535
RFR	RFE	3	PCA	2	1836.188	42.851	42.607
RFR	RFE	3	RFE	1	1267.882	35.607	35.040
RFR	RFE	3	RFE	2	1524.045	39.039	38.720
RFR	RFE	3	UNI	1	1253.850	35.410	35.360
RFR	RFE	3	UNI	2	1456.068	38.158	37.100
RFR	UNI	2	PCA	1	1881.986	43.382	42.687
RFR	UNI	2	RFE	1	1289.080	35.904	34.950
RFR	UNI	2	UNI	1	1855.248	43.073	42.590
RFR	UNI	3	PCA	1	1865.516	43.192	42.150
RFR	UNI	3	PCA	2	1781.672	42.210	41.480
RFR	UNI	3	RFE	1	1312.606	36.230	35.220
RFR	UNI	3	RFE	2	1528.714	39.099	37.490
RFR	UNI	3	UNI	1	1833.102	42.815	42.730
RFR	UNI	3	UNI	2	1514.040	38.911	36.950
Lasso	PCA	2	PCA	1	3233.305	56.862	56.559
Lasso	PCA	2	RFE	1	3233.305	56.862	56.559

Lasso	PCA	2	UNI	1	3233.305	56.862	56.559
Lasso	PCA	3	PCA	1	3233.305	56.862	56.559
Lasso	PCA	3	PCA	2	1482.972	38.509	37.888
Lasso	PCA	3	RFE	1	4240.119	65.116	63.358
Lasso	PCA	3	RFE	2	6381.702	79.886	78.418
Lasso	PCA	3	UNI	1	4240.119	65.116	63.358
Lasso	PCA	3	UNI	2	6381.702	79.886	78.418
Lasso	RFE	2	PCA	1	5145.824	71.734	71.515
Lasso	RFE	2	RFE	1	5803.548	76.181	75.782
Lasso	RFE	2	UNI	1	5803.548	76.181	75.782
Lasso	RFE	3	PCA	1	3509.574	59.242	58.900
Lasso	RFE	3	PCA	2	2450.304	49.501	49.035
Lasso	RFE	3	RFE	1	5803.548	76.181	75.782
Lasso	RFE	3	RFE	2	5821.096	76.296	75.822
Lasso	RFE	3	UNI	1	5803.548	76.181	75.782
Lasso	RFE	3	UNI	2	2183.612	46.729	45.626
Lasso	UNI	2	PCA	1	1855.364	43.074	41.857
Lasso	UNI	2	RFE	1	5803.548	76.181	75.782
Lasso	UNI	2	UNI	1	5803.548	76.181	75.782
Lasso	UNI	3	PCA	1	3509.574	59.242	58.900
Lasso	UNI	3	PCA	2	2450.304	49.501	49.035
Lasso	UNI	3	RFE	1	5803.548	76.181	75.782
Lasso	UNI	3	RFE	2	5821.096	76.296	75.822
Lasso	UNI	3	UNI	1	5803.548	76.181	75.782
Lasso	UNI	3	UNI	2	2183.612	46.729	45.626
SVR	PCA	2	PCA	1	1692.061	41.135	40.765
SVR	PCA	2	RFE	1	1692.061	41.135	40.765
SVR	PCA	2	UNI	1	1692.061	41.135	40.765
SVR	PCA	3	PCA	1	1692.061	41.135	40.765
SVR	PCA	3	PCA	2	1699.896	41.230	40.861
SVR	PCA	3	RFE	1	1766.873	42.034	41.673
SVR	PCA	3	RFE	2	1780.980	42.202	40.887
SVR	PCA	3	UNI	1	1786.889	42.272	41.899
SVR	PCA	3	UNI	2	1701.993	41.255	40.887
SVR	RFE	2	PCA	1	1720.868	41.483	41.117
SVR	RFE	2	RFE	1	1682.112	41.014	40.643
SVR	RFE	2	UNI	1	1745.169	41.775	41.412
SVR	RFE	3	PCA	1	1638.501	40.478	40.103

SVR	RFE	3	PCA	2	1689.387	41.102	40.733
SVR	RFE	3	RFE	1	1682.112	41.014	40.643
SVR	RFE	3	RFE	2	1726.821	41.555	41.189
SVR	RFE	3	UNI	1	1745.169	41.775	41.412
SVR	RFE	3	UNI	2	1683.041	41.025	40.655
SVR	UNI	2	PCA	1	1603.529	40.044	39.612
SVR	UNI	2	RFE	1	1745.169	41.775	41.412
SVR	UNI	2	UNI	1	1745.169	41.775	41.412
SVR	UNI	3	PCA	1	1638.501	40.478	40.103
SVR	UNI	3	PCA	2	1689.387	41.102	40.733
SVR	UNI	3	RFE	1	1682.112	41.014	40.643
SVR	UNI	3	RFE	2	1726.821	41.555	41.189
SVR	UNI	3	UNI	1	1745.169	41.775	41.412
SVR	UNI	3	UNI	2	1683.041	41.025	40.655